

FOR OFFICIAL USE ONLY

JPRS L/9624

24 March 1981

USSR Report

EARTH SCIENCES

(FOUO 3/81)



FOREIGN BROADCAST INFORMATION SERVICE

FOR OFFICIAL USE ONLY

NOTE

JPRS publications contain information primarily from foreign newspapers, periodicals and books, but also from news agency transmissions and broadcasts. Materials from foreign-language sources are translated; those from English-language sources are transcribed or reprinted, with the original phrasing and other characteristics retained.

Headlines, editorial reports, and material enclosed in brackets [] are supplied by JPRS. Processing indicators such as [Text] or [Excerpt] in the first line of each item, or following the last line of a brief, indicate how the original information was processed. Where no processing indicator is given, the information was summarized or extracted.

Unfamiliar names rendered phonetically or transliterated are enclosed in parentheses. Words or names preceded by a question mark and enclosed in parentheses were not clear in the original but have been supplied as appropriate in context. Other unattributed parenthetical notes within the body of an item originate with the source. Times within items are as given by source.

The contents of this publication in no way represent the policies, views or attitudes of the U.S. Government.

COPYRIGHT LAWS AND REGULATIONS GOVERNING OWNERSHIP OF MATERIALS REPRODUCED HEREIN REQUIRE THAT DISSEMINATION OF THIS PUBLICATION BE RESTRICTED FOR OFFICIAL USE ONLY.

FOR OFFICIAL USE ONLY

JPRS L/9624

24 March 1981

USSR REPORT
EARTH SCIENCES
(FOUO 3/81)

CONTENTS

METEOROLOGY

Problems in Atmospheric Optics..... 1

OCEANOGRAPHY

Bionic Modeling of Fish Electric Communication and Location Systems..... 5

Vertical Microstructure of the Thin Ocean Surface Layer..... 20

Mathematical Models of Circulation in the Ocean..... 26

Mathematical Model of General Circulation of the Atmosphere and Ocean... 28

Possibilities of Summation of Reflected Signals in Seismic Profiling
Systems..... 34

TERRESTRIAL GEOPHYSICS

Seismic Investigations of the Lithosphere in the Pacific Ocean..... 38

PHYSICS OF ATMOSPHERE

Modeling of Physical Processes in the Polar Ionosphere..... 43

- a - [III - USSR - 21K S&T FOUO]

FOR OFFICIAL USE ONLY

FOR OFFICIAL USE ONLY

METEOROLOGY

UDC 551.510:539.184

PROBLEMS IN ATMOSPHERIC OPTICS

Leningrad PROBLEMY ATMOSFERNOY OPTIKI in Russian 1979 (signed to press 8 Jun 79)
pp 191-195

[Table of contents and abstracts from collection "Problems in Atmospheric Optics",
edited by A. L. Osherovich, Izdatel'stvo Leningradskogo universiteta, 1000 copies,
196 pages]

[Text]

TABLE OF CONTENTS

Pavlova, V. S. "Sergey Fedorovich Rodionov".....	3
Kondrat'yev, K. Ya. (Leningrad University) "Present-Day Climate and Factors Determining It".....	11
Rozenberg, G. V. (Institute of Atmospheric Physics USSR Academy of Sciences) "Origin of the Atmospheric Selective Transparency Effect".....	21
Khrgian, A. Kh. (Moscow University) "On the Theory of Glow Phenomena".....	25
Bol'shakova, L. G., (Leningrad University) "Allowance for the Width of the Spec- tral Interval in Measurements of the Vertical Distribution of Ozone in the Atmosphere".....	40
Sulakvelidze, G. K. (Tbilisi University) "Some Problems in the Growth of Hail in a Cloud".....	63
Osherovich, A. L., Verolaynen, Ya. F. (Leningrad University) "Method of Delayed Coincidences in Atomic and Molecular Spectroscopy".....	80
Fishkova, L. M. (Abastumani Astrophysical Observatory Academy of Sciences Georgian SSR) "Nighttime Emission of Sodium in the Earth's Upper Atmosphere".....	154
Bol'shakova, L. G. (Leningrad University) "Decimal Coefficients of Rayleigh Scattering of the Standard Atmosphere in the Spectral Region 200-400 nm Each 0.4 nm".....	172
Georgiyevskiy, Yu. S., Shukurov, A. Kh. (Institute of Atmospheric Physics USSR Academy of Sciences) "Variations in the Spectral Coefficient of Attenuation of Radiation by Atmospheric Aerosol in the UV Spectral Region".....	180

FOR OFFICIAL USE ONLY

Pavlova, Ye. N. (Leningrad University) "Size of Selectively Scattering Particles of Atmospheric Aerosol Over El'brus"..... 187

Abstracts

UDC 551.583.13

PRESENT-DAY CLIMATE AND FACTORS DETERMINING IT

[Abstract of article by Kondrat'yev, K. Ya.]

[Text] A study was made of the problem of the possible effect exerted on climate by factors related to variations of ozone and atmospheric aerosol. The author emphasizes the important role of satellite observations of different parameters determining the climate of the planet.

UDC 551.593.6

ORIGIN OF THE ATMOSPHERIC RELATIVE TRANSPARENCY EFFECT

[Abstract of article by Rozenberg, G. V.]

[Text] The author discusses the theory of the selective atmospheric transparency effect discovered by S. F. Rodionov. The correctness of the interpretation of the observed facts proposed by S. F. Rodionov is demonstrated.

UDC 551.593.55

ON THE THEORY OF GLOW PHENOMENA

[Abstract of article by Khrgian, A. Kh.]

[Text] The possible spectral effects of light scattered by a layer of stratospheric aerosol at an altitude of 20 km at twilight are examined. It is shown that such scattering can create a red or yellow spot over the setting sun with a distinct lower limb and a diffused upper limb. This gives an explanation for the observed purple light and some other glow phenomena.

UDC 551.510.534

ALLOWANCE FOR THE WIDTH OF THE SPECTRAL INTERVAL IN MEASUREMENTS OF THE VERTICAL DISTRIBUTION OF OZONE IN THE ATMOSPHERE

[Abstract of article by Bol'shakova, L. G.]

[Text] A method for computing the vertical distribution of ozone on the basis of ozonsonde data is described for a case when narrow-band light filters are used. A quantitative evaluation of the accuracy of the method is presented.

FOR OFFICIAL USE ONLY

UDC 551.509.616/617

SOME PROBLEMS IN THE GROWTH OF HAIL IN A CLOUD

[Abstract of article by Sulakvelidze, G. K.]

[Text] It is shown that the growth of hail occurs for the most part due to coagulation with the supercooled accumulated large-droplet fraction. The conditions under which the creation of artificial hail nuclei can limit their growth to $R_0 \leq 0.55$ cm are evaluated. The number of collisions of hailstones with supercooled droplets, leading to their growth, is computed. It is shown that the number of collisions is a function of the concentration of supercooled droplets in the cloud and their size distribution.

UDC 539.184

METHOD OF DELAYED COINCIDENCES IN ATOMIC AND MOLECULAR SPECTROSCOPY

[Abstract of article by Osherovich, A. L., Verolaynen, Ya. F.]

[Text] The article describes one of the most universal and precise methods for investigating the excited states of atoms and molecules -- the delayed coincidences method. The accuracy of the method is evaluated. It is shown that the delayed coincidences method can be used in investigating the elementary processes of populating and destruction of energy levels.

UDC 550.388

NIGHTTIME EMISSION OF SODIUM IN THE EARTH'S UPPER ATMOSPHERE

[Abstract of article by Fishkova, L. M.]

[Text] The article presents the results of systematic observations (from 1958 to 1970) of sodium emissions ($\lambda_1 = 589.0$ nm and $\lambda_2 = 589.6$ nm) in the earth's nighttime sky obtained using a photoelectric photometer at the Abastumani Astrophysical Observatory. A study was made of the diurnal, seasonal and annual variations of this emission. The theory of the observed patterns is discussed.

UDC 551.510.534

DECIMAL COEFFICIENTS OF RAYLEIGH SCATTERING OF THE STANDARD ATMOSPHERE IN THE SPECTRAL REGION 200-400 nm EACH 0.4 nm

[Abstract of article by Bol'shakova, L. G.]

[Text] The article gives the results of computation of the volume coefficients of Rayleigh scattering for a vertical column of the atmosphere with a base 1 cm^2 each 0.4 nm in the spectral region of ozone absorption from 200 to 400 nm.

FOR OFFICIAL USE ONLY

FOR OFFICIAL USE ONLY

UDC 551.510.42:551.521.3

VARIATIONS IN THE SPECTRAL COEFFICIENT OF ATTENUATION OF RADIATION BY ATMOSPHERIC AEROSOL IN THE UV SPECTRAL REGION

[Abstract of article by Georgiyevskiy, Yu. S., Shukurov, A. Kh.]

[Text] The results of measurements of spectral transparency and the spectral coefficients of attenuation of radiation by atmospheric aerosol on slant and horizontal paths are presented and discussed. It is shown that the main influence on atmospheric transparency in the UV and visible spectral regions is exerted by particles with a radius of about $0.3\mu\text{m}$, whose concentration correlates with air humidity.

UDC 551.521.3

SIZE OF SELECTIVELY SCATTERING PARTICLES OF ATMOSPHERIC AEROSOL OVER EL'BRUS

[Abstract of article by Pavlova, Ye. N.]

[Text] An estimate of the radius of selectively scattering particles in the air layer at an altitude of 3-3.2 km over the glacier in the El'brus region is given. It is shown that the radius of the aerosol particles can vary from $0.2\mu\text{m}$ over firn fields to $1.23\mu\text{m}$ over the valley.

COPYRIGHT: Izdatel'stvo Leningradskogo universiteta, 1979
[76-5303]

5303
CSO: 1865

FOR OFFICIAL USE ONLY

FOR OFFICIAL USE ONLY

OCEANOGRAPHY

BIONIC MODELING OF FISH ELECTRIC COMMUNICATION AND LOCATION SYSTEMS

Moscow VESTNIK AKADEMII NAUK SSSR in Russian No 1, Jan 81 pp 99-110

[Article by V. M. Ol'shanskiy, A. A. Orlov, and Dr Biol Sci V. R. Protasov]

[Text] The methods of creating bionic models differ from methods usually employed in biological research to model any processes or phenomena. Every biological object is typified, on one hand, by universality in relation to the functions it performs and, on the other hand, unique features inherent only to a living organism. Using technical devices to directly copy biological structures performing certain functions fails to produce optimum solutions. Therefore when building a bionic model, it would be best to use only the general phenomenological characteristics typifying a particular aspect of the activity or function of a living organism, applying in this case the sum total of presently available knowledge and technical devices.

Information on Electric Fish

About 300 of the 20,000 presently existing fish species possess special electricity generating tissues and are capable of generating electric fields. Among these, only the electric eels, electric catfish, electric skates, and American stargazers have distinctly pronounced electric organs with which they create intense electric fields about themselves, used in attack or defense. The electric organs of the skate, for example, generate discharges having an amplitude of up to 50 w and a current intensity of up to 50 amp in sea water. The energy of such a discharge may be estimated as 1 mj per gram of electric organs. The frequency of discharges in response to stimulation attains 150 Hz, each discharge lasting 3-5 msec.

The rest of the species make up a second group of so-called weakly electric fish, which generate relatively weak electric fields with amplitudes on the order of 5-10 w in water.

Weakly electric fish are divided in terms of the sort of discharges generated into wave and pulsating species. Pulsating species include all Mormyriiformes (except for gymnarchids) and the bulk of the gymnotids. The duration of discharges produced by pulsating species is much shorter than the time interval between discharges; in this case the fish may vary the discharge frequency within broad limits. For most pulsating species, this range is 1-60 pulses/sec. Wave species generate

FOR OFFICIAL USE ONLY

FOR OFFICIAL USE ONLY

quasisinusoidal discharges of practically constant frequency. These frequencies are species-specific, and they fall within the 50-2,000 Hz range.

Fields generated around fish differ from electric fields around dipole sources (Figure 1) mainly due to nonuniform distribution of a fish's electric skin resistance.

The electric organs of fish consist of specialized cells (electric plates) transformed, as a rule, out of muscle fibers and, in some species, out of nerve fibers. A typical feature of these cells is functional differentiation of cell membranes, taking the form of innervation of just one side. At the moment of stimulation, the potential difference across an electric plate attains 40-120 mv. Electric plates in electric organs are stacked into columns, which are in turn connected in parallel. Owing to this the emf and current produced by the whole electric organ significantly exceed the corresponding outputs of a single electric plate. The orientation of these columns in electric organs located in the fish body predetermines the polarity of the discharge and the current direction.

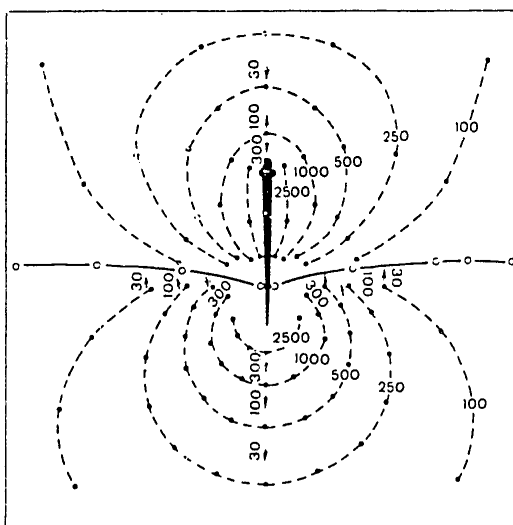


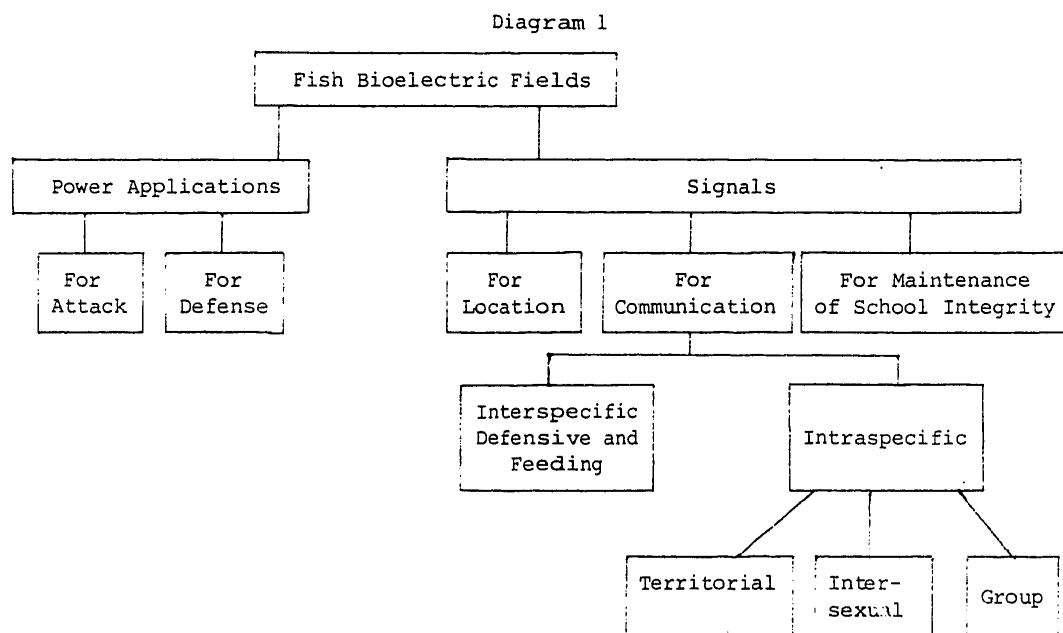
Figure 1. Electric Field of a 22 cm Long *Apteronotus* in Water With Specific Resistance Equal to $3.2 \text{ kohm} \cdot \text{cm}$ (From Knudsen, E. I., "Spatial Aspects of the Electric Fields Generated by Weakly Electric Fish," JOURN. COMP. PHYSIOL., Vol 99, 1975, pp 103-118): Field potentials are indicated horizontally in μv on the equipotential lines corresponding to them. Field intensities are indicated vertically in $\mu\text{v}/\text{cm}$ near the vectors associated with them.

All weakly electric and many strongly electric species have electroreceptors exhibiting high electric sensitivity. They evolved from fish lateral line organs, and they are situated in the skin, communicating to the body surface through pores.

FOR OFFICIAL USE ONLY

Their density is usually greatest in the anterior parts of the body and the head. In terms of their physiological properties, electroreceptors are divided into two basic types--tonic and phasal. Tonic electroreceptors adapt slowly, and they are sensitive to low frequency electric fields in the 0.5-20 Hz range. Receptors of this type have also been found among both freshwater and marine electric fish, as well as among some nonelectric species. Phasal electroreceptors have been found only in freshwater weakly electric species and in the electric eel. These quickly adapting high frequency receptors exhibit their greatest sensitivity in the 60-2,000 Hz range--that is, in the frequency range of electric organ discharges.

The joint operation of electric organs and electroreceptors of weakly electric fish supports electrolocation and electrocommunication functions. Because tonic electroreceptors are insensitive to the discharges of electric organs, their basic purpose is apparently associated with so-called passive location and orientation--that is, with registration of external electric fields of biotic and abiotic origin. The ways fish use their bioelectric fields in their vital activities are diagrammed below (Diagram 1).



Modeling Electrocommunication Systems

The principal carrier frequencies of the discharges of the electric organs of weakly electric fish are species-specific as a rule, and therefore we can hypothesize that electric fields are used by fish mainly for intraspecific communication. Experiments have demonstrated the existence of electrocommunication in a large number of weakly electric fish, and that such communication has dominant significance in sexual and territorial mutual relationships. The range of electrocommunication detected by R. Bauer in experiments with a 15 cm long *Gnathonemus petersii* is

FOR OFFICIAL USE ONLY

30 cm, which agrees with the theoretical estimate of this value for most weakly electric species.

Investigation of fish electrocommunication requires thorough physico-technical analysis of close electromagnetic low frequency communication in conducting media. Without clear physico-technical premises, we cannot perform competent experiments, theoretically predict the possibilities of fish electrocommunication systems, reveal the mechanisms of their operation, adequately describe the parameters of electrocommunication systems, and assess their optimum parameters from different points of view. Moreover it would doubtlessly be interesting to develop electroconductive communication devices of direct practical significance. From a historical standpoint, most pioneering efforts in this direction were started under the influence of ideas suggested in the biological literature.

Examining the problems associated with short-range underwater electrocommunication, we should distinguish the following physico-technical aspects:

propagation of electromagnetic fields in conducting media; effectiveness of transmitting and receiving antennas, and matching antennas to the apparatus; factors restricting transmission and reception possibilities; design of the system as a whole--selection of the operating frequency and type of modulation, estimation of the range and dependability of communication in relation to given overall dimensions of the apparatus and its power supply possibilities, and so on.

Let us examine these problems briefly.

Propagation

In most technical situations, the required ranges of communication significantly exceed the necessary depths of communication. It would be advantageous in this case to select the working frequency of communication such that the electromagnetic signals would propagate as a so-called "surface wave", which may be arbitrarily imagined as a signal propagating upward from its source to the water surface, then through air along the surface and, finally, downward through water to the receiver. The nature of propagation is basically defined as the product of two terms:

$$\frac{1}{r^3} \quad \text{and} \quad \frac{-z+h}{e^{\delta}}$$

where r --range of communication, $z+h$ --total depth of communication, δ --magnitude of skin layer in water. Approximations describing propagation of an electromagnetic field in practically all real communication situations have been published.*

* Bannister, P. R., "Quasi-Static Fields of Dipole Antennas at the Earth's Surface," RADIO SCI., Vol 1, No 11, 1966, pp 1321-1330; Kraichman, M. B., "Handbook of Electromagnetic Propagation in Conducting Media," NAVMAT, 1970.

FOR OFFICIAL USE ONLY

In biological and some technical applications, meanwhile, the surface wave assumption (the assumption that the total depth of the source and receiver is much less than the range of communication) is unacceptable. In these cases the simplest approximation is used in the estimates as a rule--equations for the field of a dipole source in a boundless, uniform conducting medium.

In a conducting medium (in distinction from dielectric media), the polar diagrams of a dipole source may be plotted only on the condition that the orientation of the receiving antenna is determined. The receiver's polar diagram may also be plotted only on the condition that the coordinates of the reception point relative to the source and the magnitude of the skin layer at the operating frequencies in water are given. At ranges from the source commensurate with the magnitude of the skin layer in water, elliptical polarization of the electric field's intensity vector is significant, and the polar diagram does not possess a zero point, no matter what the orientation of the receiving dipole antenna in the polarization plane.

Assessment of Antenna Effectiveness

An electric dipole source can be fully described by the dipole moment Il . If we represent Il as

$$Il = \sqrt{\frac{P}{|z_e|}} \cdot l = \sqrt{\alpha_e P},$$

where P --power, z --total impedance, and l --effective antenna length, coefficient $\alpha_e = l^2/(|z_e|)$ may be used as a measure of the effectiveness of an electric dipole antenna: Of two identically situated and identically oriented antennas of equal power, that having the greater α_e will emit the greater signal at any distant point.

If the class of antennas is given, we can optimize them--that is, we can find the antenna with the greatest α_e . For example in the class of dipole antennas with a fixed total length L , those antennas having electrodes with longitudinal dimensions on the order of $1/3L$ are optimum.

α_e may be increased by placing an insert made from insulating or fully conducting material between the electrodes. This raises the effective length of the antenna.

α_e may be used to assess the effectiveness of dipole antennas in terms of not only emission but also reception: The greater α_e is, the greater is the signal to noise ratio. However, this is valid only if two conditions are observed:

the length of the receiving antenna is much less than the range of communication;

The sensitivity of the receiver depends on the antenna's thermal noise, and not some other factors (for example the level of atmospheric disturbances).

FOR OFFICIAL USE ONLY

There are many practical situations in which these conditions are not satisfied. Such situations require development of ways to suppress outside interference; therefore it would be suitable to use multi-electrode antennas, which would require subsequent correlation processing of the recorded potentials (recall that the number of electroreceptors in fish is very large). Multi-electrode antennas require a fundamentally new approach to assessment of the effectiveness of receiving antennas. Developing such an approach is a pressing problem of engineering and bionics.

The Electromagnetic Background

The electromagnetic background in water is the product of sources of different origins (Diagram 2). Each component in the diagram may dominate under certain conditions. However, at the frequencies used for underwater electrocommunication, fields produced by thunderstorms (atmospheric disturbances) are dominant as a rule. A large number of papers devoted to them not only cite experimental data but also thoroughly analyze the origin and propagation of atmospheric disturbances.* A knowledge of the theory of atmospheric disturbances permits us to approximate experimentally measured levels and spectrums at other depths, explain the temporal and spatial features of the background, and predict the unique features of the given region. It is important to study the electromagnetic background both from the standpoint of practical engineering problems and from the standpoint of biological problems (electro-ecological in particular). Investigation of fields of biological origin is an important part of the study of electromagnetic fields in water.

The Design of Concrete Electrocommunication Systems

In contrast to the situation with most known communication systems (radio, acoustic, optical), the design and parameters of underwater electrocommunication devices depend to a significant extent on the concrete application, and as a rule, if communication is to be maintained with a different object, a new device of a different sort would have to be developed. Designing such devices entails determining the communication frequency (f), signal intensity (E_0) at the reception point required for communication, and transmitter power (P); the most suitable types and designs of antennas are revealed, and their u_0 are computed. If the particular communication problem is fundamentally soluble, the dependability of communication may be assessed with a consideration for the possible mutual orientations of the transmitting and receiving antennas. The computations are usually made in several stages, in each of which the values of the parameters and the designs are narrowed down more specifically.

We will go through the motions of making a tentative assessment of the operating frequency of communication as an illustration of the whole computation process.

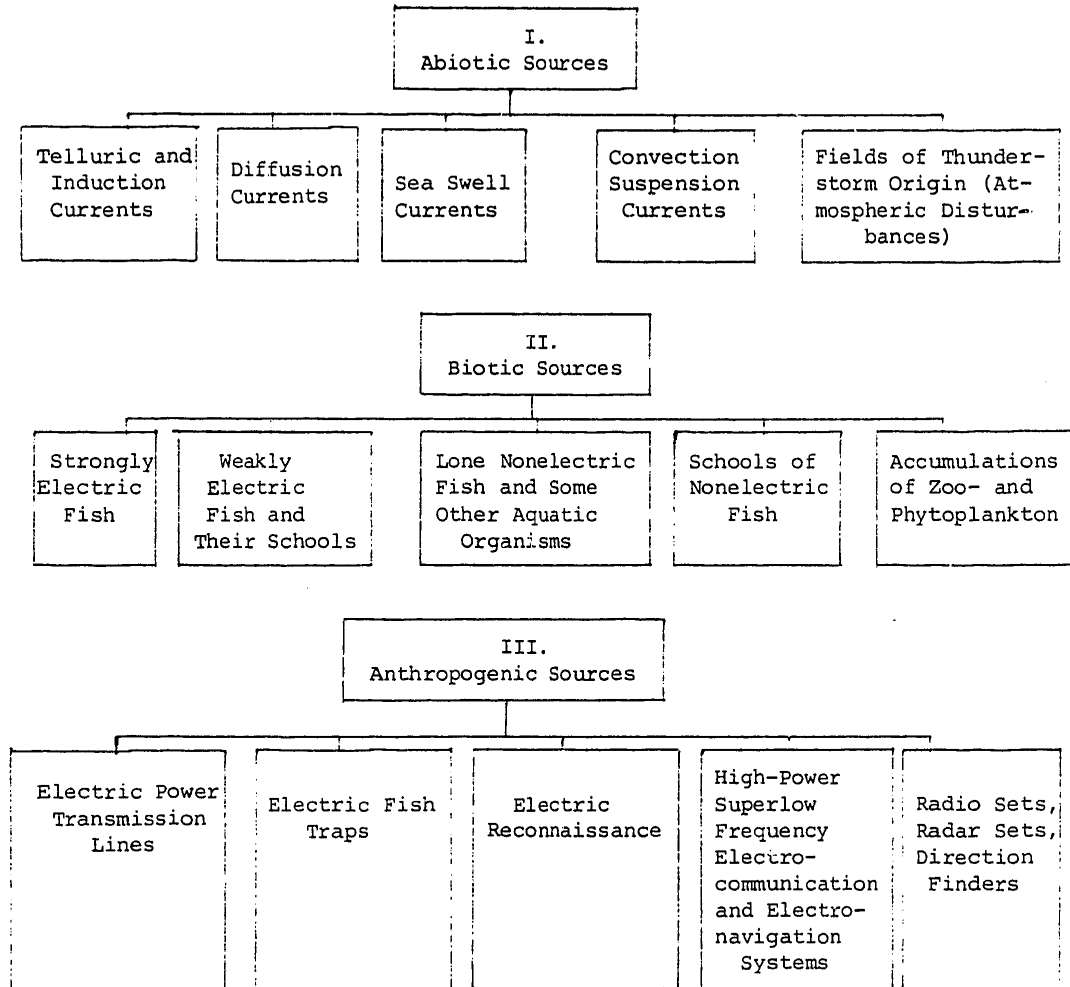
Because there is an exponential term in the equations for propagation in a conducting medium, electromagnetic communication is impossible at frequencies at which

* Maxwell, E. L., "Atmospheric Noise From 20 Hz to 30 kHz," JOURN. RES. NBS, Vol 2, No 6, 1967.

FOR OFFICIAL USE ONLY

FOR OFFICIAL USE ONLY

Diagram 2
Sources of Electric Fields in an Aquatic Environment



the depth of the skin layer in the medium is significantly lower than the range of communication (or, in the case of a surface wave, lower than the total depth of the source and receiver).

On the other hand the low information content typical of communication at low frequencies and the usually observed decrease in the level of the electromagnetic

FOR OFFICIAL USE ONLY

FOR OFFICIAL USE ONLY

background in water in response to growth in frequency indicate to us that it would be unsuitable to use frequencies so low that the depth of the skin layer in the medium would significantly exceed the range of communication (or, correspondingly, the total depth of the source and receiver).

Consequently it would be suitable to select the operating frequency such that the maximum communication range would be equivalent to several (three to five for example) skin layers in water. Correspondingly, in the case of a surface wave the operating frequency must be such that the total depth of the receiving and transmitting apparatus would be equivalent to two or three skin layers. Thus if commands must be transmitted from a vessel to fishing gear located up to 400 meters below the surface in ocean water, the specific electroconductivity of which is $4 \text{ ohm}^{-1} \text{ m}^{-1}$, then, considering that a skin layer of 100 meters corresponds here to a frequency of 18 Hz, we can recommend this frequency as the one to be used.

In addition to these considerations, when selecting the operating frequency of communication we also account for the nature of the signal (for example, speech), the need for suppressing the industrial frequency (50 or 60 Hz) and its harmonics, and the possibilities and convenience of practical realization of the device. Thus if we are dealing with weakly electric fish communicating in fresh water (the specific electroconductivity of which is about $10^{-1} \text{ ohm}^{-1} \text{ m}^{-1}$) at ranges on the order of several meters, frequencies on the order of hundreds of MHz would be the most advantageous. But the known frequency range used by weakly electric fish does not exceed units of kHz, which is apparently associated with the difficulties of achieving high frequencies in biological structures.

We computed the parameters for several concrete systems on the basis of these considerations.

They included a shipboard device to control apparatus mounted on a trawl (Figure 2), a system permitting communication among SCUBA divers (Figure 3), and "shore-to-water" and "water-to-air" communication systems. The computation results were checked out by natural experiments conducted in the Sea of Japan. The parameters of the systems are presented below.

For the shipboard device controlling apparatus mounted on a trawl: communication range--1 km, depth--up to 400 meters, operating frequencies--10-16 Hz, dipole moment--10,000 amp·m.

For electrocommunication between SCUBA divers: communication range--70 meters, depth--up to 50 meters, operating frequencies--300 Hz to 2 kHz, dipole moment--2 amp·m.

For "water-to-air" communication: communication range--200 meters, transmitter depth--50 meters, altitude of reception point--70 meters, communication frequency--300 Hz, dipole moment--7.5 amp·m.

For "shore-to-water" communication: communication range--2 km, communication depth--50 meters, working frequencies--16 Hz to 2 kHz, dipole moment--1,000 amp·m.

These devices are now being introduced for practical use.

FOR OFFICIAL USE ONLY

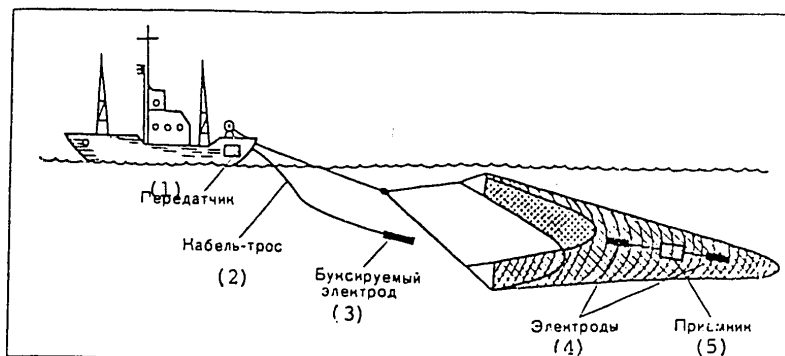


Figure 2. Shipboard Device Controlling Apparatus Mounted on a Trawl

Key:

- | | |
|--------------------|---------------|
| 1. Transmitter | 4. Electrodes |
| 2. Cable | 5. Receiver |
| 3. Towed electrode | |

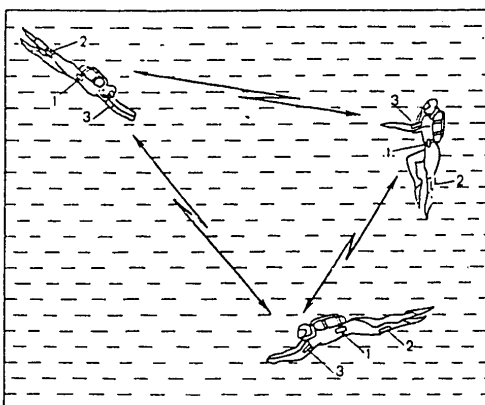


Figure 3. Electrocommunication Between SCUBA Divers: 1--apparatus, 2--leg-mounted electrode, 3--shoulder-mounted electrode

FOR OFFICIAL USE ONLY

FOR OFFICIAL USE ONLY

Discussing the prospects and limitations of bionic modeling of fish electro-communication systems, we should point out the following basic differences between these systems and the underwater electrocommunication devices known today.

Biological electrocommunication involves distances commensurate with the dimensions of the object involved. At the location of a receiving partner, the electric field is significantly nonuniform, and it is picked up by a large quantity of electroreceptors located all over the body of the fish. In a technical application, meanwhile, communication entails distances significantly exceeding the dimensions of the object involved, the field near the receiving partner is quasiuniform, and the signal is picked up by dipole antennas. Fuller utilization of the spatial structure of a signal and interference, and transition to dipole antennas from multi-electrode receivers would be promising from the standpoint of solving the most important problems of underwater electrocommunication, such as raising the information content of communication, raising the signal to noise ratio, improving electromagnetic compatibility, and improving interaction with other systems (electric location and orientation systems).

On the other hand, in distinction from the situation in the biological world, technical applications permit the use of components with specific electroconductivity significantly exceeding the specific electroconductivity of water--components made of superconducting metals. Such components make it possible to employ concepts that are inapplicable to living nature--that is, ones outside the scope of bionic modeling.

Modeling Electrolocation Systems

Active electrolocation is defined as registering changes in the electric field produced by weakly electric fish due to distortion of this field by objects characterized by conductivity different from the conductivity of the surrounding medium. Almost all known weakly electric fish of both wave and pulsating species have an electrolocation capability. It should be noted in this case that the two basic taxonomic groups of weakly electric fish--African Mormyriiformes and South American gymnotids--reside in the turbid waters of rivers and streams. The capability for detecting and discriminating between objects by means of an electric field is a remarkable adaptation of a living organism to an environment in which conventional visual orientation is difficult and often impossible. This is precisely why a fish's electrolocation system, which to some extent substitutes for the animal's vision, represents a new sensory system--"electrovision".

The electrolocation function was first discovered in 1958 by G. Lissmann and K. Meychin in a representative of the African Mormyriiformes, *Gymnarchus niloticus*. Using a conditioned reflex technique, the scientists revealed that the fish are capable of distinguishing between metallic and dielectric objects enclosed in porous cases, and distinguishing between fresh and salt water contained in these cases. It was also demonstrated that the distribution of the potential of the electric field on the surface of the fish's skin, created by electric organ discharges, becomes distorted when objects having electroconductivity different from that of water come near the fish body. It was hypothesized that channel-like structures located in the skin--mormyromasts--are responsible for picking up

FOR OFFICIAL USE ONLY

FOR OFFICIAL USE ONLY

these distortions, and thus that they are electroreceptors--a new class of sensory units discovered among representatives of the animal world. Numerous studies subsequently performed* in this direction were devoted to the physiology and morphology of electroreceptors and electric organs, as well as to the principles and mechanisms of their joint work.

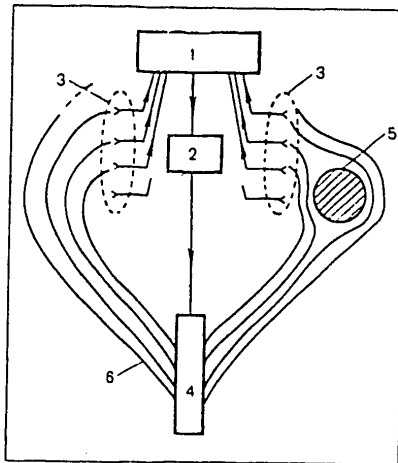


Figure 4. Active Electrolocation: 1--central nervous system, 2--electric organ command (triggering) center, 3--electroreceptors, 4--electric organ, 5--object of detection, 6--electric field flux lines

Figure 4 provides a general diagrammatic approximation of active electrolocation. The field generated by the electric organ and distortions within it are picked up by phasal electroreceptors located in the fish's skin (the density of electroreceptors in some species attains 80 per square millimeter). Then information is successively transmitted by a system of nerve tracts to different divisions of the central nervous system. In addition to processing signals structurally associated with the lateral lobes of the medulla oblongata, the central nervous system monitors the work of the command center controlling the electric organ. There are intracentral associations directly associated with the electrolocation function. One of them manifests itself as avoidance of jamming signals by changing the fundamental carrier frequency of the electric organ's discharges.

Electroreceptor systems participating in active location must react in the best way possible not to the electric field itself but to changes within it, thus manifesting a capability for so-called relative sensitivity. The general functional characteristics of any electroreceptor are:

passive conduction of electric current through the tissues of the electroreceptor to the surface of the receptor cell;

*Bennett, M. V. L., "Electric Organs. Electroreception," in Hoar, W. S., and Randall, D. J. (Editors), "Fish Physiology," New York, 1971; Protasov, V. R., "Bioelektricheskiye polya v zhizni ryb" [Bioelectric Fields in the Life of Fish], Moscow, 1972; Heiligenberg, W., "Principles of Electrolocation and Jamming Avoidance in Electric Fish," Berlin-Heidelberg-New York, Springer-Verlag, 1977.

FOR OFFICIAL USE ONLY

the activity of the receptor cell itself, expressing itself as generation of a reception potential and synaptic transmission of a stimulus to nerve endings;

the capability for encoding signals in a form convenient for subsequent transmission by an afferent fiber.

An adequate stimulus acting upon a receptor would consist of a potential difference between the opening of the receptor pore on the skin surface and the basal membrane of the receptor cell. The mechanism of action of the receptor is as follows: Current generated either by an outside source or by the electric organ itself first passes through the highly conductive tissues of the channel, and then through the apical nonconductive membrane of the receptor cell, which acts as a high frequency filter, and through the basal membrane. If the voltage drop across it reaches the absolute threshold, the cell generates a regenerative receptor potential, which is responsible for activation of the nerve fiber innervating the cell. This activity carries information on gradual changes in the electric current passing through the receptor, and it is responsible for one of the types of codes carried by the fiber.

Mention should be made of the great diversity of information encoding methods (four or five basic types are conditionally distinguished) correlating approximately with this type of electroreceptor. The advantages of a particular type of encoding used by fish are to a great extent hypothetical, though they are discussed in detail in many papers. Incidentally, the large number of functional types of electroreceptor units is obviously associated with the need for differentiating their properties so as to permit their use in electrolocation and electrocommunication. In this case even receptor units intended solely for location are characterized by different adaptation times in relation to a varying stimulus, which indicates that they are predisposed for detecting either motionless or moving objects. Some phasal electroreceptors (the *T*-units of gymnotids) exhibit so-called phasal sensitivity--that is, they respond differently to stimuli, producing either an ohmic or a capacitive load of the same impedance. This is believed to be associated with the capability fish have for identifying plant and animal objects which, as we know, have significant capacitive properties.

Electrosensory information undergoes primary processing in the lateral lobes of the medulla oblongata, when signals from a tremendous number of receptors covering the entire surface of the animal's body experience temporal and spatial integration. Just at the level of the lateral lobes, a fish's sensitivity to objects rises by about one order of magnitude in comparison with the sensitivity of a single electroreceptor, which agrees with data from conditioned reflex experiments performed to determine the threshold sensitivity of fish.

We can conditionally distinguish two directions in contemporary research on fish electrolocation systems. The first concerns itself with the spatial aspects of electrolocation and deals with the following problems:

investigation and numerical modeling of the geometry of fields generated by electric organs, and fields associated with introduced objects;

study of the spatial orientation of the electroreceptors with the purpose of revealing how important it is to assessment of the dimensions of an object and the range to it, and to precise determination of the object's conductive properties.

FOR OFFICIAL USE ONLY

The second direction is associated with the temporal aspects of electrolocation. It deals with the following problems:

clarification of the way the rate or frequency of electric organ discharge affects whether or not the electrolocation system is optimum;

investigation of the ways and means of functional differentiation of electroreceptor units permitting their simultaneous participation in electrolocation, using a single processing center in this case;

study of the electrolocation capability of fish in the presence of noise.

The advances that have been made in both directions provide a sufficiently full impression of the general peripheral phenomenology of fish electrolocation systems, and thus allow us to construct its bionic model. It is also obvious that further study of the mechanisms and principles of information processing in the central nervous system will make it possible to significantly update this model.

In its physical interpretation, the problem of modeling fish electrolocation systems boils down to building an electrolocation system which can detect an object on the basis of the amount of distortion it creates in the primary electric field, and to seeking optimum circuits for the emitting and receiving devices. For practical purposes this problem should be divided into two. The first concerns close-range electrolocation, or "electrovision", which permits detailed identification of the object, to include its structure, shape, and dimensions. Certain advances have already been made in this direction in our country by A. I. Bondarchuk (Minsk Radiotechnical Institute), but the resolution of his system is satisfactory only when the array of measuring electrodes is located right next to the object. The second problem, which will be examined below, consists of building a model capable of detecting objects at greater range. The first step in this problem is to try to formalize the basic principle of electrolocation, so as to permit sensitive assessment of the object size which the model could detect and the ranges within which it can function.

Simple mathematical expressions may be obtained, for example, for the case of a metal ball located within the field of a dipole emitter (Figure 5). If the distance \bar{d} from the emitter to the object is much greater than the length \bar{l} of the dipole and the diameter $2a$ of the ball being detected, a dipole approximation may be used to describe the field of the emitter, and near the object the field itself may be assumed to be uniform. If, moreover, the object is located on the axis of the emitting dipole, then the intensity of the distorting field at the location of the emitting antenna is

$$E_r = \frac{Il}{2\pi\alpha_1} \cdot \frac{a^3}{d^3}$$

In order to register the maximum difference of potentials, the measuring electrodes must obviously be located as far apart as possible. But because the entire

FOR OFFICIAL USE ONLY

electrolocation model must obviously be contained within the same carrier and occupy a limited volume, the maximum spread between the measuring electrodes would have to be limited to the length l of the emitting dipole. In this case the maximum potential difference bearing information about the object is

$$U_1 = I \frac{a^3 l^2}{2\pi\sigma_1 d^3}$$

Thus if prior to introduction of the object the potential difference at the emitting electrodes was U (assuming no change in current), then after the object is introduced, we observe an increment in the potential difference across the electrodes, U_1 , which depends on the dimensions of the object and the distance to it. It is easy to see that the term

$$\frac{a^3 l^2}{2\pi\sigma_1 d^3}$$

has electric resistance as its unit, and the inclusion of an object in the circuit of the emitting electrode changes the external load R , defined by the value of interelectrode resistance, by the amount

$$dR = \frac{a^3 l^2}{2\pi\sigma_1} \cdot \frac{1}{d^3}$$

Similar expressions may be obtained for any solid having a shape different from spherical.

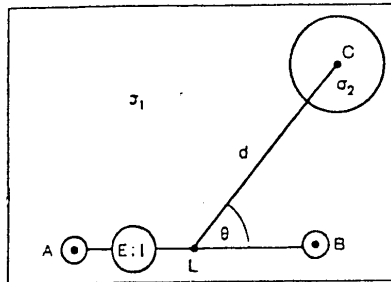


Figure 5. Emitting Electrodes A and B, Separated by Distance L , are Contained in the Circuit of a Generator With an emf of E : I --current in the emitting circuit; a spherical object of detection with radius a and its center at point C is separated from the emitting dipole by distance d ; θ --angle between dipole axis and a radius-vector extended from the center of the dipole to point C ; σ_1, σ_2 --specific electroconductivity of the medium and the object

FOR OFFICIAL USE ONLY

In addition to a useful component bearing information on the object, dR would also include all sorts of noise-producing fluctuations in electric resistance. They include:

Fluctuations in interelectrode resistance occurring due to temperature changes in the medium, changes in salinity, and so on;

noise-caused changes in electrode resistance associated with instability of the double electric layer and fluctuations of electric potential;

noise produced by the motion of water masses, particularly by waves on the water surface.

The expression for U may thus be rewritten as:

$$U_1 = I \left(\frac{a^2 l^2}{2\pi\sigma_1 d^3} + dR' \right),$$

where dR' represents the total noise-caused fluctuations of impedance. In this case the maximum possible electrolocation range would be defined by the ratio dR/dR' , and it would not be affected by an increase in the power of the system, as is the case in electrocommunication. In order to plan and tentatively assess the possibilities of an electrolocation system, we would need to know the values of all known noise parameters, and account for them.

One of the first systems based on this principle is a highly simple electrolocation system* intended for installation aboard small vessels and yachts. Such a system is capable of detecting underwater obstacles within a range equivalent to 1.5-3 vessel lengths, and determining the direction of their movement.

Research aimed at improving this electrolocation system involves theoretical and experimental determination of all noise components. From the design aspect, this means seeking optimum electrode systems characterized by minimum impedance fluctuations.

As far as the prospects of bionic modeling of fish electric systems in general are concerned, electrocommunication models are now the nearest to immediate practical use in this vast area, and the most enticing direction is that of creating "electro-vision", which would have great significance not only to engineering but also to biology, cybernetics, and medicine.

* See Swain, W. H., "An Electric Field Aid to Underwater Navigation" in "IEEE Int. Conf. on Engineering in Ocean Environment. Panama, Florida," Vol 1, 1970, pp 122-124.

COPYRIGHT: Izdatel'stvo "Nauka", "Vestnik Akademii nauk SSSR", 1981
[161-11004]

11004
CSO: 1840

FOR OFFICIAL USE ONLY

UDC 551.465.63

VERTICAL MICROSTRUCTURE OF THE THIN OCEAN SURFACE LAYER

Moscow DOKLADY AKADEMII NAUK SSSR in Russian Vol 256, No 3, 1981 pp 694-698

[Article by N. V. Vershinskiy, Yu. A. Volkov and A. V. Solov'yev, Institute of Physics of the Atmosphere USSR Academy of Sciences, manuscript submitted 2 Jul 80]

[Text] One of the tasks of the 29th voyage of the scientific research ship "Akademik Kurchatov," carried out under the international FGGE program, was an investigation of the vertical structure of the thin surface layer of the Atlantic Ocean. In the investigation use was made of a probe of a special design making measurements as it rises to the surface [1,2]. Such a method makes it possible to obtain the vertical distributions of the investigated characteristics near the ocean surface with minimum disruptions of natural conditions.

The probe was supplied with a low-inertia temperature sensor and a sensor of fluctuations of conductivity. The time constant of the temperature sensor was about 3 msec, which corresponds to approximately 3 mm vertically with a rate of movement of the probe in a working regime of 1 m/sec. The resolution of the conductivity sensor was 1 mm. The mean square noise level during the time of one sounding (~10 sec) was 0.0006°C for the temperature channel and $5 \cdot 10^{-5}$ mho/m for the conductivity channel. The zero drift of the temperature sensor between individual soundings was $\pm 0.05^\circ\text{C}$. The conductivity sensor, due to the peculiarities of its design, made it possible to register only relative changes in conductivity.

The measurements were made in July-August 1979 in two regions of the tropical zone of the Atlantic Ocean: in the intertropical convergence zone (ICZ) and at the equator, in the zone of Trades circulation.

In the ICZ region a substantial influence of rain on the vertical structure of the thin surface layer was registered when there was a weak wind. During periods of calm weather intensive solar heating here frequently alternated with heavy rain. At the ocean surface there was formation of layers of freshened (lighter) water, making difficult turbulent exchange with the lower-lying water mass. In combination with intensive solar heating this led to the formation of sharp density drops. In the surface layer there was a rather complex pattern of vertical stratification.

The results of investigation of the patterns of daytime heating of the surface layer of the ocean in the presence of a weak wind and in the absence of a rain [2-4], as well as the availability of detailed information on the vertical distributions

FOR OFFICIAL USE ONLY

FOR OFFICIAL USE ONLY

particular, Fig. 1b,c shows the vertical temperature distributions obtained at 1418 and 1802 hours respectively. The thickness of the daytime quasihomogeneous layer at 1418 hours was about 0.4 m. The vertical temperature gradient at a depth of 0.4 m attained $15^{\circ}\text{C}/\text{m}$. In the evening there was a deepening of the daytime quasihomogeneous layer and a decrease in the temperature drop forming due to daytime heating (Fig. 1c).

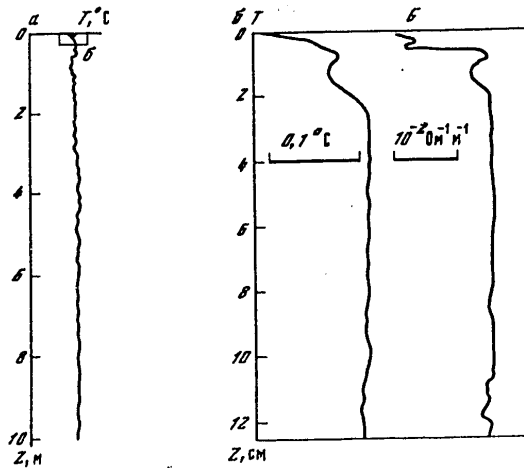


Fig. 2. Vertical structure of the thin surface layer of the ocean under nighttime cooling conditions in the presence of a weak wind.

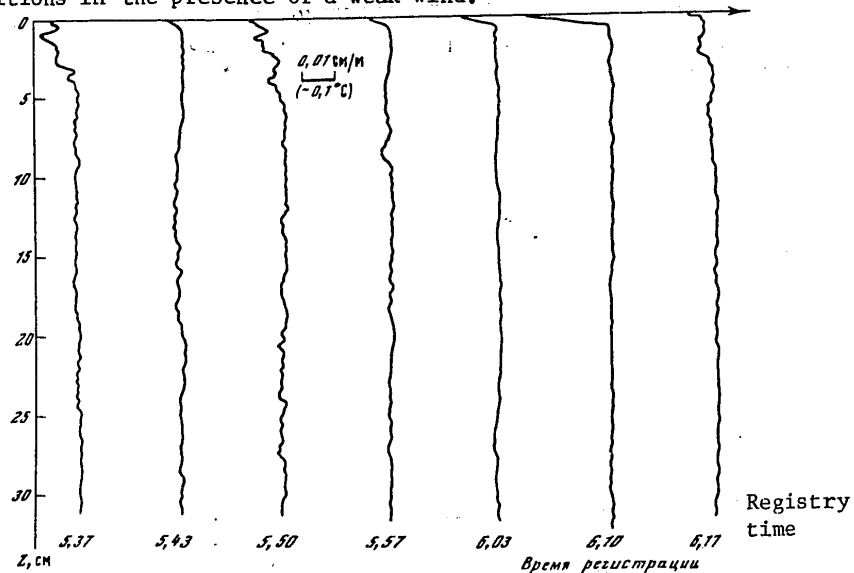


Fig. 3. Series of vertical distributions of conductivity near the ocean surface under conditions of nighttime cooling in the presence of a weak wind.

FOR OFFICIAL USE ONLY

In the layer 3.3-4.2 m (Fig. 1a) there is a temperature inversion, evidently forming as a result of nighttime convective cooling of the above-lying freshened layer. The unstable temperature stratification in this layer is more than compensated by the stable salinity stratification and therefore the corresponding distribution of conditional density is stable.

In the layer with an inverse temperature distribution (3.3-4.2 m) there can be development of layered convection due to the effects of double diffusion of heat and salt [5]. This sector is shown at a more expanded scale in the lower part of Fig. 1a. A stepped structure is rather clearly seen here in the vertical distribution of salinity.

Stable Trade winds predominated during measurements in the equatorial polygon (July-August). With a wind force not greater than 3 scale units near the ocean surface there was formation of a very thin daytime quasihomogeneous layer and the thermocline at its lower boundary. Corresponding conditions for this phenomenon in the equatorial polygon (wind force < 3 scale units) were observed during almost 34% of the total time in July and 10% in August.

At nighttime when there is a weak wind near the ocean surface the formation of discrete convective elements was observed. This phenomenon was investigated thoroughly in laboratory experiments ([6,7] and others), but evidently was observed for the first time under the natural conditions of the ocean.

Figure 2a illustrates one of the series of vertical temperature distributions in the 10-m surface layer of the ocean obtained at nighttime on 11 August 1979 in the equatorial polygon (01°40'N, 18°51'W). At the time of these measurements the wind velocity was $U \approx 3$ m/sec. The total heat flow from the ocean surface was $Q_{surf} \approx -170$ W/m²; the heat flow due to evaporation was $Q_L \approx -90$ W/m². The vertical temperature distribution revealed the presence of weak unstable stratification in the upper meters, which was associated with cooling of the ocean through its free surface.

Figure 2b shows the vertical temperature distribution in the uppermost part of the water layer and a synchronous record of the vertical distribution of conductivity. These records evidently registered the moment of formation of a discrete convective element in the upper centimeters of the ocean surface layer.

The vertical temperature distributions near the free surface of the water during the formation of a thermal obtained in a laboratory experiment [7] had a similar form.

The vertical structure of the upper centimeters (Fig. 2b) was traced in particular detail in the conductivity channel, having, as already noted, a better spatial resolution than the temperature channel.

The application of the Monin-Obukhov similarity theory [8] to the surface layer of the ocean makes it possible to evaluate the characteristic scales of temperature T^* and salinity S^* changes:

$$[\pi = surf] \quad T^* \approx -Q_n / c_p \rho U_* \quad S^* \approx F / \rho U_*$$

FOR OFFICIAL USE ONLY

where U_* is friction velocity in the water; $F = -(S/\lambda)Q_L$ is the salt flux due to evaporation; S is salinity; λ is the specific heat of evaporation; c_p, ρ are specific heat capacity and water density respectively. For the dimensions of inhomogeneities greater than the internal scales of turbulent disturbances of temperature η_T and salinity η_S [5] the ratio of the characteristic changes of conductivity due to temperature ΔG_T and due to salinity ΔG_S has the following form (in the absence of freshening of the surface layer due to rain):

[$\pi = \text{surf}$]

$$\Delta G_T / \Delta G_S \approx \beta_T T_s / \beta_S S_s = \beta_T \lambda Q_n / \beta_S c_p S Q_L,$$

where

$$\beta_T = (\partial G / \partial T)_{S,p}, \beta_S = (\partial G / \partial S)_{T,p}.$$

For the conditions observed during the measurements, for example, on the night of 11 August 1979 in the equatorial polygon, the ratio $\Delta G_T / \Delta G_S = 25$, $\eta_S \approx 0.07$ mm, $\eta_T \approx 0.7$ mm (the η_S and η_T evaluations are somewhat exaggerated due to the fact that only the generation of turbulence due to buoyancy forces was examined).

Accordingly, in this case the changes in conductivity for scales greater than 1 mm for the most part must be related to temperature changes. These evaluations give basis for using the vertical conductivity distributions for an analysis of the thermal structure of the surface layer of the ocean during nighttime convection.

Figure 3 shows a series of 7 vertical distributions of conductivity obtained during the dark time of day. The wind velocity during the measurements was $U \approx 2$ m/sec and the heat flows from the ocean surface were $Q_{\text{surf}} \approx -120$ W/m², $Q_L \approx -60$ W/m². The observed variability of the vertical distribution of conductivity in the upper centimeters of the ocean surface layer is in accordance with the phenomenological theory of free convection with large Rayleigh numbers [9].

Here, however, it must be taken into account that the period of cyclic convective processes near the ocean surface for our case should be ~ 40 sec [9, 10] and the horizontal scale should be about 1 cm [9]. The minimum time interval between two successive soundings was several minutes. The drift of the vessel between two successive soundings was tens of meters. Therefore, in each sounding there was registry of the vertical structure of a cyclic convective process in some random stage.

An analysis of the vertical distributions is somewhat difficult due to the fundamental peculiarities of operation of the conductivity sensors near the water-air discontinuity. In our case the vertical microstructure was conveyed without distortions beginning at a depth of 2 mm. Accordingly, the sector of vertical distributions of conductivity in the depth range from 0 to 2 mm was excluded from consideration and is not shown in the figures.

The vertical distributions obtained at 0543, 0603 and 0610 hours (Fig. 3) can be interpreted as the stage of formation of the thermal boundary layer by means of the molecular diffusion of heat. The thickness of this layer attained about 8 mm in the vertical distribution obtained at 0610 hours. The vertical distributions obtained at 0537 and 0550 hours evidently belong to the stage of a convective surge destroying the forming thermal boundary layer. The vertical distributions obtained at 0557 and 0617 hours can be assigned to the stage of attenuation of the

FOR OFFICIAL USE ONLY

FOR OFFICIAL USE ONLY

convective surge and the onset of formation of a new thermal boundary layer by means of the molecular diffusion of heat.

The results of investigations of the fine structure in the tropical region of the Atlantic Ocean confirmed the data available earlier for other regions [2,4]. New data were obtained on the influence of rain on the microstructure of the surface layer of the ocean. In addition, evidently for the first time in the ocean there was registry of formation of discrete convective elements near the surface at nighttime.

The authors express appreciation to V. V. Turenko for developing the electronic circuitry of a conductivity sensor and to K. N. Fedorov and A. I. Ginzburg for valuable comments.

BIBLIOGRAPHY

1. Vershinskiy, N. V., Solov'yev, A. V., OKEANOLOGIYA (Oceanology), Vol 17, No 2, 1977.
2. Vershinskiy, N. V., Nelepo, B. A., Solov'yev, A. V., DAN (Reports of the USSR Academy of Sciences), Vol 247, No 3, 1979.
3. Solov'yev, A. V., Vershinskiy, N. V., DAN, Vol 240, No 5, 1978.
4. Solov'yev, A. V., IZV. AN SSSR, FIZ. ATM. I OKEANA (News of the USSR Academy of Sciences: Physics of the Atmosphere and Ocean), Vol 15, No 7, 1979.
5. Fedorov, K. N., TONKAYA TERMOKHALINNAYA STRUKTURA VOD OKEANA (Fine Thermohaline Structure of Ocean Waters), Leningrad, Gidrometeoizdat, 1976.
6. Sparrow, E. M., Husar, R. B., Goldstein, R. I., J. FLUID MECH., Vol 41, 793, 1970.
7. Ginzburg, A. I., Zatsepin, A. G., Fedorov, K. N., IZV. AN SSSR, FIZ. ATM. I OKEANA, Vol 13, No 12, 1977.
8. Monin, A. S., Yaglom, A. M., STATISTICHESKAYA GIDROMEKHANIKA (Statistical Hydro-mechanics), Part 1, Moscow, "Nauka," 1965.
9. Foster, T. D., GEOPHYSICAL FLUID DYNAMICS, Vol 2, p 201, 1971.
10. Ginzburg, A. I., Golitsyn, G. S., Fedorov, K. N., IZV. AN SSSR, FIZ. ATM. I OKEANA, Vol 15, No 3, 1979.

COPYRIGHT: Izdatel'stvo "Nauka", "Doklady Akademii nauk SSSR", 1981
[87-5303]

5303
CSO: 1865

FOR OFFICIAL USE ONLY

UDC 551.465.11

MATHEMATICAL MODELS OF CIRCULATION IN THE OCEAN

Novosibirsk MATEMATICHESKIYE MODELI TSIRKULYATSII V OKEANE in Russian 1980 (signed to press 19 May 80

[Annotation and table of contents from monograph edited by G. I. Marchuk, academician, and A. S. Sarkisyan, doctor of physical and mathematical sciences, Izdatel'stvo "Nauka", Sibirskoye Otdeleniye, 1250 copies, 288 pages]

[Text] Annotation. This monograph is devoted to the theory and methods of mathematical modeling of oceanic circulations developed at the Computation Center of the Siberian Department USSR Academy of Sciences. A number of formulations of the problem of ocean dynamics are considered, their resolution is investigated and effective algorithms are proposed for their realization. Much attention is devoted to difference schemes and methods for solving the formulated problems. The results of computations of hydrothermodynamic fields are given and analyzed for individual seas and oceans and for the world ocean as a whole. The book is of interest for specialists working in the field of computational mathematics, hydrodynamics, oceanology and meteorology.

TABLE OF CONTENTS

Foreword..... 3

Chapter 1. Mathematical Problems of Dynamics of the Stratified Ocean..... 6

 1.1. Linear model of a baroclinic ocean..... 7

 1.2. Nonlinear models of a baroclinic ocean..... 17

 1.3. Stabilization of solutions of linear problems in ocean dynamics..... 32

Chapter 2. Mathematical Modeling of the Thermocline and Vertical Turbulent Exchange in the Ocean..... 44

 2.1. On the problem of formation of the thermocline in the ocean..... 44

 2.2. Turbulent energy equation..... 50

 2.3. Equation of dissipation of turbulent energy..... 54

 2.4. Determination of empirical constants..... 57

Chapter 3. Numerical Methods for Solving Problems in Macroscale Movements in the Ocean..... 64

 3.1. Principal approaches to formulation of discrete models of ocean dynamics 64

 3.2. Modeling of barotropic and baroclinic ocean currents..... 67

 3.3. Numerical methods for solving nonstationary equations of ocean thermodynamics..... 101

 3.4. Difference schemes for solving problems in dynamics of a baroclinic ocean..... 120

FOR OFFICIAL USE ONLY

Chapter 4. Increase in the Order of Approximation of Difference Schemes for Equations of Ocean Dynamics..... 135

4.1. Increase in the order of approximation by the embedded grids method.... 136

4.2. Exclusion of schematic viscosity by the successive approximations method..... 144

4.3. Solution of equation for level surface..... 148

4.4. Difference scheme for equation of density diffusion with stipulated fluxes at boundary..... 152

4.5. Computation of difference solution gradients..... 156

Chapter 5. Spectral Methods for Solving Problems in Ocean Dynamics..... 161

5.1. Some problems in formulating spectral models of ocean dynamics..... 161

5.2. Formulation of problem of dynamics of tides of a barotropic world ocean..... 162

5.3. Formulation of finite-difference approximations..... 164

5.4. Formulation of spectral problem for difference analogue of tidal operator..... 166

5.5. Method of simultaneous iterations for solving the partial spectral problem..... 167

5.6. Inverse iterations method for solving the problem of free oscillations. 170

5.7. Spectral method for solving the equations of dynamics of a baroclinic world ocean..... 174

Chapter 6. Circulation of Waters of the World Ocean..... 180

6.1. Concise review of new foreign investigations of this problem..... 180

6.2. Model of thermohydrodynamics of the world ocean..... 183

6.3. Model of global circulation on basis of finite elements method..... 193

6.4. Modeling of macroscale fields of density and currents in the world ocean..... 203

Chapter 7. Investigation of Patterns of Macroscale Circulation in the Example of Individual Seas and Oceans..... 216

7.1. Ekman boundary layer..... 216

7.2. Upper quasihomogeneous layer in a three-dimensional model of ocean circulation..... 226

7.3. Modeling of macroscale density fields in North Atlantic..... 238

7.4. Investigation of formation of hydrological characteristics in ocean... 247

7.5. Numerical model of dynamics and thermal regime of Lake Baykal..... 256

Notations Employed..... 273

Bibliography..... 274

Subject Index..... 285

COPYRIGHT: Izdatel'stvo "Nauka", 1980
[69-5303]

5303
CSO: 1865

FOR OFFICIAL USE ONLY

UDC 551.46

MATHEMATICAL MODEL OF GENERAL CIRCULATION OF THE ATMOSPHERE AND OCEAN

Moscow DOKLADY AKADEMII NAUK SSSR in Russian Vol 253, No 3, 1980 pp 577-581

[Article by G. I. Marchuk, academician, V. P. Dymnikov, V. B. Zalesnyy, V. N. Lyk-
osov, N. M. Bobyleva, V. Ya. Galin and V. L. Perov, Computation Center, Siberian
Department USSR Academy of Sciences, Novosibirsk, manuscript submitted 6 Mar 80]

[Text] The problem of creating mathematical models of general circulation of the
atmosphere and ocean is evidently one of the central problems in solving the
problem of long-range forecasting of weather and climate and its change. In this
article we examine a three-dimensional model of circulation of the atmosphere and
ocean is one of the possible variants implemented on the basis of a complex of al-
gorithms and programs developed at the Computation Center USSR Academy of Sciences.
This complex makes it possible to formulate models with different levels of com-
plexity: atmospheric circulation with a stipulated temperature at the ocean sur-
face [1], oceanic circulation with a stipulated temperature at its surface [2],
atmospheric circulation with involvement of the upper quasihomogeneous layer of
the ocean [3], etc.

1. The system of differential equations describing the joint macroscale circulation
of the atmosphere and ocean is conveniently represented in the form of two main
parts describing atmospheric and oceanic movements respectively. The equations of
atmospheric hydrothermodynamics are formulated in a spherical coordinate system
 $O\lambda\varphi\sigma$ (the σ -coordinate is used vertically [1, 3])

$$\begin{aligned} \frac{du}{dt} - \left(1 + \frac{u}{a} \operatorname{tg} \varphi\right) v + \frac{1}{a \cos \varphi} \left(\frac{\partial \Phi}{\partial \lambda} + \frac{RT}{\pi} \frac{\partial \pi}{\partial \lambda}\right) &= \frac{F_u}{\pi}, \\ \frac{dv}{dt} + \left(1 + \frac{u}{a} \operatorname{tg} \varphi\right) u + \frac{1}{a} \left(\frac{\partial \Phi}{\partial \varphi} + \frac{RT}{\pi} \frac{\partial \pi}{\partial \varphi}\right) &= \frac{F_v}{\pi}, \\ \frac{\partial \pi}{\partial t} + \frac{1}{a \cos \varphi} \left(\frac{\partial \pi u}{\partial \lambda} + \frac{\partial \pi v \cos \varphi}{\partial \varphi}\right) + \frac{\partial}{\partial \sigma} \pi \dot{\sigma} &= 0, \quad \frac{\partial \Phi}{\partial \sigma} + \frac{RT}{\sigma} = 0, \end{aligned} \quad (1)$$

FOR OFFICIAL USE ONLY

FOR OFFICIAL USE ONLY

$$\frac{dT}{dt} - \frac{RT}{c_p \sigma} \left[\pi \dot{\sigma} + \sigma \left(\frac{\partial \pi}{\partial t} + \frac{u}{a \cos \varphi} \frac{\partial \pi}{\partial \lambda} + \frac{v}{a} \frac{\partial \pi}{\partial \varphi} \right) \right] = \frac{F_T}{\pi} + \epsilon, \quad (1)$$

$$\frac{dq}{dt} = \frac{F_q}{\pi} - (C - E),$$

$$\dot{\sigma} = 0, \quad \Phi = \Phi_S \text{ with } \sigma = 1, \quad \dot{\sigma} = 0 \text{ with } \sigma = 0. \quad (2)$$

In the λ, φ coordinates use is made of the condition of periodicity of the solution

$$u = u^0, \quad v = v^0, \quad \pi = \pi^0, \quad T = T^0, \quad q = q^0|_{t=0}. \quad (3)$$

The model of dynamics of the ocean [4] is formulated in a spherical coordinate system $O\lambda\varphi z$:

$$\begin{aligned} \frac{\partial u}{\partial t} - lu &= \frac{1}{a \cos \varphi} \frac{\partial p}{\partial \lambda} + \frac{\partial}{\partial z} \nu \frac{\partial u}{\partial z} + F_\lambda, \\ \frac{\partial v}{\partial t} + lv &= -\frac{1}{a} \frac{\partial p}{\partial \varphi} + \frac{\partial}{\partial z} \nu \frac{\partial v}{\partial z} + F_\varphi, \quad \frac{\partial p}{\partial z} = g\rho, \end{aligned} \quad (4)$$

$$\frac{1}{a \cos \varphi} \left(\frac{\partial u}{\partial \lambda} + \frac{\partial v \cos \varphi}{\partial \varphi} \right) + \frac{\partial w}{\partial z} = 0 \text{ at } \Omega$$

$$\frac{dT}{dt} = \frac{\partial}{\partial z} \nu_T \frac{\partial T}{\partial z} + \mu_T \Delta T, \quad \rho = \rho(T).$$

The boundary conditions are:

$$u = v = \dot{w}, \quad \frac{\partial T}{\partial n} = 0 \quad \text{in } S_n,$$

$$w = 0, \quad \nu \frac{\partial u}{\partial z} = -\frac{\tau_N}{\rho_0}, \quad \nu \frac{\partial v}{\partial z} = -\frac{\tau_\varphi}{\rho_0} \quad \text{with } z = 0, \quad (5)$$

$$\nu_T \frac{\partial T}{\partial z} = Q_T, \quad w = \frac{dH}{dt}, \quad \nu \frac{\partial u}{\partial z} = -R \int_0^H u dz, \quad \nu \frac{\partial v}{\partial z} = -R \int_0^H v dz,$$

$$\frac{\partial T}{\partial n_1} = 0 \quad \text{with } z = H, \quad (6)$$

$$u = u^0, \quad v = v^0, \quad T = T^0 \quad \text{with } t = 0.$$

The notations used here and the form of the operators and functions on the right-hand sides of (1), describing the processes of radiation, convective and phase influxes of heat, as well as the dissipation and diffusion of energy in the

FOR OFFICIAL USE ONLY

atmosphere, are given in [1-4]; we note only that Ω in (4) is a cylindrical region of determination of the solution (4)-(6) with a lower base equal to the intersection of the surfaces $\{\sigma = 1\} / \{z = 0\}$ and the lateral surface S_n .

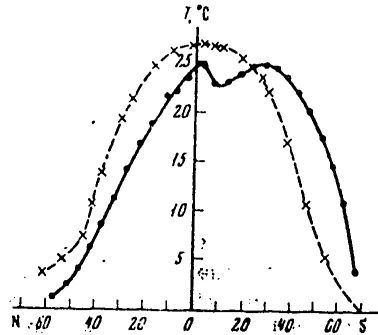


Fig. 1. Zonally averaged distribution of ocean surface temperature. The solid curve gives the results of computations; the dashed curve represents actual data.

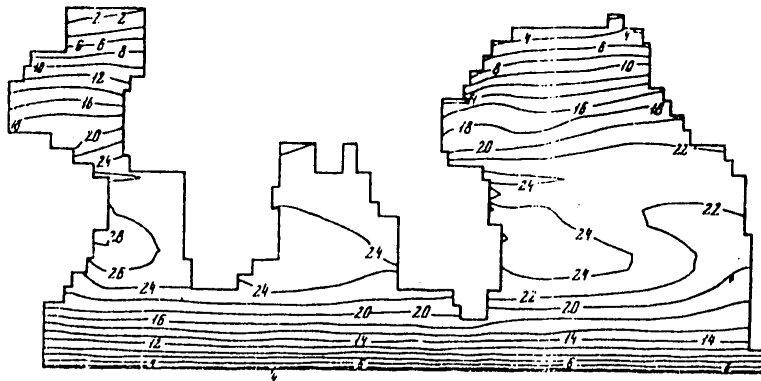


Fig. 2. Temperature of ocean surface. Results of computations.

Interacting with one another, the atmosphere and ocean exchange heat, moisture and moment of momentum. The temperature at the ocean surface is computed from the thermodynamic equation; it is assumed that the upper quasihomogeneous layer in the ocean has a constant depth ~ 100 m. The heat flux from the atmosphere into the ocean is determined as the residual term in the equation for the heat balance at the ocean surface, including the terms describing the radiation balance, turbulent flux of heat into the atmosphere and expenditures of heat on evaporation. Since in this experiment no consideration was given to the equations of dynamics of salinity

FOR OFFICIAL USE ONLY

FOR OFFICIAL USE ONLY

in the ocean, in the mechanism for the exchange of moisture between the atmosphere and ocean we took into account only the terms describing the moisture flux from the ocean surface into the atmosphere and the flow of moisture from the land into the ocean. The exchange of the moment of momentum occurred by the use of the components of the surface frictional stress, computed in the atmospheric model, as the upper boundary condition for the equations of ocean dynamics. The method proposed in [5] was used for the artificial synchronization of the times of thermal relaxation of the atmosphere and ocean.

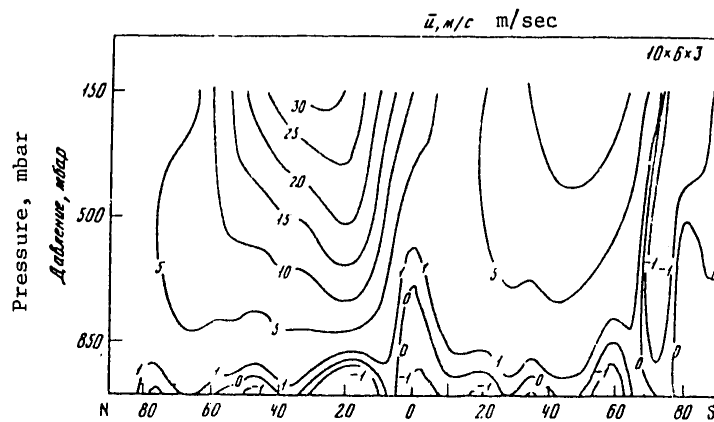


Fig. 3. Zonally averaged u-component of velocity vector.

3. The numerical algorithm for the solution of problem (1)-(6) is based on use of its finite-difference discretization in space variables and a combination of two types of the splitting method for application in the time coordinate. The selected strategy for solution of the problem, having a number of advantages from the point of view of effectiveness and stability of the computations relative to the usually employed algorithms [5, 6], imposes more rigorous limitations on the properties of the discrete analogue of the problem operator (for example, the properties of skew-symmetry or positive determinability of the difference operators in each splitting interval). Adherence to these requirements will increase the stability of the global computation system and the choice of the time integration interval in this case is related only to the natural approximation conditions. In the model successive use is made of the method of splitting with respect to physical processes and in geometric coordinates. In this connection systems (1-3) and (4-6) are reduced to a systematized evolutionary form [4]. In each time interval there is separate examination of the transfer and adaptation (splitting with respect to physical processes) equations; in the transfer stage use is made of further splitting of the three-dimensional operator of the problem in space variables.

4. A numerical experiment was carried out for computing the joint circulation of the atmosphere and ocean with input data corresponding to the winter period for the northern hemisphere. Mean January solar declination, the boundary of sea ice, cloud albedo and albedo of the ocean surface were stipulated. The smoothed relief

FOR OFFICIAL USE ONLY

FOR OFFICIAL USE ONLY

of the earth's surface was introduced. The computational parameters of the model were: in the atmosphere $\Delta t = 40$ min, $\Delta \lambda = 10^\circ$, $\Delta \varphi = 6^\circ$, 3 levels in the σ -coordinate; in the ocean $\Delta t = 2$ days, $\Delta \lambda = \Delta \varphi = 5^\circ$, 4 levels in the z -coordinate. The experiment consisted of two stages. First with a fixed temperature at the ocean surface we separately computed atmospheric and oceanic circulation for the periods corresponding to quasi-equilibrium regimes in the atmosphere and ocean and then we carried out computations of the joint circulation for 11 "oceanic" years, which for the atmosphere is a time of about two months. We will cite some results of a numerical experiment.

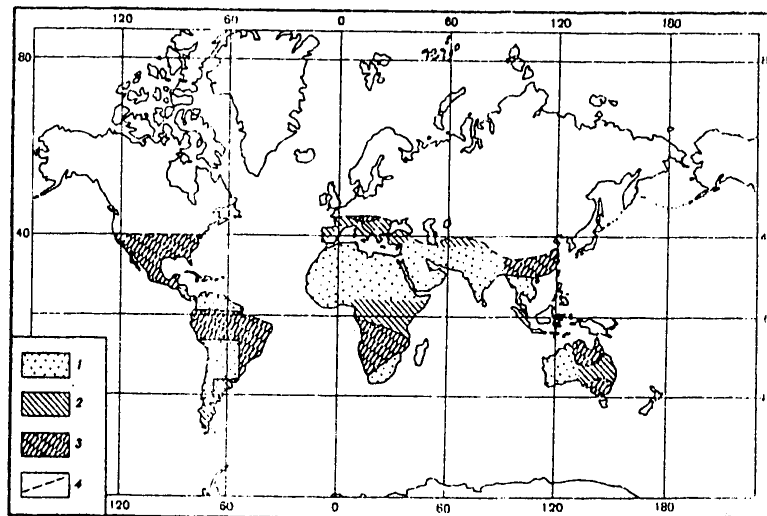


Fig. 4. Distribution of moisture reserves in the soil (W): 1) $W < 0.5$ cm; 2) $0.5 \leq W \leq 5$ cm; 3) $W > 5$ cm; 4) snow line.

The principal parameter determining the influence of the ocean on atmospheric circulation, as is well known, is the temperature of the ocean surface. Figure 1 shows the zonally averaged distribution of ocean surface temperature obtained as a result of computations (solid curve) and constructed on the basis of actual data (dashed curve). The field of ocean surface temperature is shown in Fig. 2. It can be seen that as a result of the computations there was found to be a general cooling of the ocean in the northern hemisphere and in the tropics and heating in the middle and southern latitudes of the southern hemisphere. A result was a decrease in the latitudinal gradient and temperature in the atmosphere, which led to reduced energy values in the long-wave region. We note the local minimum of ocean surface temperature in the tropics caused by the equatorial upwelling. The distributions of temperature, humidity and dynamic characteristics in the atmosphere are quantitatively extremely similar to the distributions obtained during the modeling of the atmosphere with a fixed temperature at the ocean surface [1].

FOR OFFICIAL USE ONLY

FOR OFFICIAL USE ONLY

We should note some decrease in the eddy flows of heat, moisture and moment of momentum in a poleward direction and the southward displacement of the tropical zone of precipitation by approximately 10° , caused by the displacement of the surface temperature maximum. As an example, Figures 3 and 4 show the zonally averaged field of the zonal wind component and the resulting distribution of moisture reserves in the soil. It is easy to note that the model as a whole reproduces well the arid and moistened zones on the continents. It is interesting to note that India is reproduced as an arid region since the winter monsoon does not carry moisture. In general it can be assumed that the model reproduces quite well the principal climatic characteristics of the real atmosphere and ocean and can be used for the purposes of study of the physical principles of climate and its changes.

BIBLIOGRAPHY

1. Marchuk, G. I., Dymnikov, V. P., et al., IZV. AN SSSR, FAO (News of the USSR Academy of Sciences: Physics of the Atmosphere and Ocean), Vol 15, No 5, 467, 1979.
2. Marchuk, G. I., Zalesnyy, V. B., SB. NAUCHN. TR. VTs SO AN SSSR (Collection of Scientific Papers, Computation Center Siberian Department USSR Academy of Sciences), Novosibirsk, 3, 1964.
3. Marchuk, G. I., Dymnikov, V. P., et al., World Meteorological Organization, Conference on Climate Models, Washington, 318, 1978.
4. Marchuk, G. I., Dymnikov, V. P., et al., GIDRODINAMICHESKAYA MODEL' OBSHCHEY TSIRKULYATSII ATMOSFERY I OKEANA (Hydrodynamic Model of General Circulation of the Atmosphere and Ocean), Novosibirsk, 1975.
5. Bryan, K., J. COMP. PHYS., Vol 4, No 3, 347, 1969.
6. Manabe, S., Brayan, K., KLIMAT I TSIRKULYATSIYA OKEANA (Climate and Ocean Circulation), Leningrad, Gidrometeoizdat, 1972.

COPYRIGHT: Izdatel'stvo "Nauka", "Doklady Akademii nauk SSSR", 1980
[8144/0722-5303]

5303
CSO: 8144/0722

FOR OFFICIAL USE ONLY

UDC 550.834

POSSIBILITIES OF SUMMATION OF REFLECTED SIGNALS IN SEISMIC PROFILING SYSTEMS

Moscow OKEANOLOGIYA in Russian Vol 21, No 1, Jan-Feb 1981 pp 180-182

[Article by G. N. Lunarskiy, Institute of Oceanology imeni P. P. Shirshov USSR Academy of Sciences, manuscript submitted 14 Dec 79, resubmitted after revision 21 Apr 80]

[Text]

Abstract: The article briefly describes the circuits of summing amplifiers for systems for single-channel continuous seismic profiling. The amplifiers ensure the summing of signals from two strings of piezoelectric detectors towed on different sides of the ship, which makes possible some increase in the signal-to-noise ratio.

Single-channel continuous seismic profiling (CSP) has come into wide use due to the high degree of mobility and the relative simplicity of the systems ensuring operation by this method. Despite the diversity of CSP systems, they have much in common, which unifies them and leads to a greater similarity of the methodological peculiarities related to operation. The different modifications of the systems differ from one another for the most part with respect to the type of source of elastic wave pulses and the electric current source employed. The receiving parts of the systems to a considerable extent are the same [1-3, 5, 6].

The advantage of single-channel systems for continuous seismic profiling is that their use is possible on many ships without imposing special requirements on them (presence of special equipment, etc.). It is possible to use virtually any ships having sufficient room for the placement of the component parts of the system and having appropriate sea-going qualities.

At the same time, the possibility of extensive use of continuous seismic profiling systems has its peculiarities associated with the characteristics of the vessel and operating conditions. For example, many vessels have a limited range of speeds or their operation is disadvantageous at a reduced speed when the continuous seismic profiling system can ensure maximum efficiency (depth of penetration). Under such conditions interference can have a high level and be caused by different factors. In this case reference is to the influence of interference associated with working mechanisms on the ship and towing of the strings of piezoelectric detectors.

FOR OFFICIAL USE ONLY

FOR OFFICIAL USE ONLY

In order to lessen the influence of these factors and increase the signal-to-noise ratio (which leads to an increase in the effective depth of the investigations) in many cases special measures must be taken. In addition to the use of vibration absorbers, shock-absorbing elements, special materials, fairings, booms, etc., use is sometimes made of a reception system consisting of two strings of piezoelectric detectors with identical parameters which are towed on different sides of the ship and at different distances from it.

The signals from the two strings of piezoelectric detectors are summed by means of special amplifiers whose electrical circuits are shown below. One of them is constructed using a microcircuit and the other is constructed using ordinary components.

In the circuit which is shown in Fig. 1 summation is accomplished using transformers whose secondary windings are appropriately connected. This circuit has low resistances and provides for the use of strings of piezoelectric detectors in which a matching transformer is used [3].

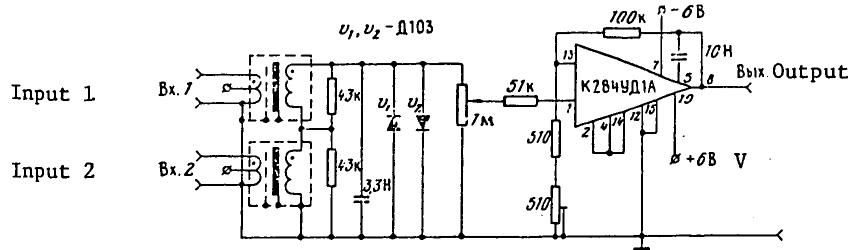


Fig. 1. Electrical circuit of summing amplifier with low-resistance inputs ensuring possibility of balancing the connecting lines from the strings of piezoelectric detectors.

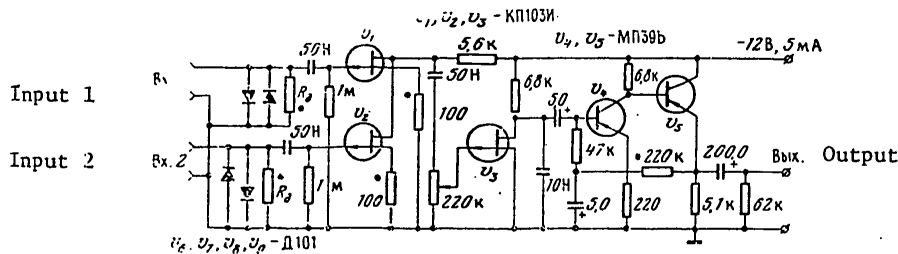


Fig. 2. Electrical circuit of summing amplifier whose input resistances can vary in a wide range.

FOR OFFICIAL USE ONLY

The primary windings of the transformers are symmetric, which ensures the possibility of use of a symmetric line (cable) for connecting strings of piezoelectric detectors with the recording apparatus. In some cases this makes it possible to reduce the background of the interference associated with induction from force fields created by electrical equipment and the ship's apparatus. With balancing of the input the midpoint of the primary winding is connected to the housing. Figure 1 shows an asymmetric input. A screen is placed between the transformer windings. The transformer parameters are dependent on the data for the matching transformer, which is placed in the string of piezoelectric detectors. In this case the transformation ratio is selected equal to 10. The presence of transformers at the amplifier input makes the circuit very responsive to external fields and therefore a good magnetic screen is required. The secondary windings are connected in series with allowance for the summation of signals coinciding in frequency and phase. A capacitor is cut in for lessening the influence of high-frequency induction. Protection of the circuit against damage in the event of random arrival of great voltages at the amplifier input is ensured by means of diodes. An operational amplifier (K284UD1A) ensures the necessary additional amplification. The required amplification level is established by means of feedback resistors. The summator pass-band with the data indicated in the circuit is 30-2500 Hz. The upper frequency is limited by a correcting capacitor of the operational amplifier, whereas the lower frequency is determined by the parameters of the input transformers of the summator and the characteristics of the string of piezoelectric detectors.

The total amplification with the feeding of cophasal signals with a frequency of 100 Hz to the input, taking into account the transfer coefficients of the transformers, is 2000. The noise voltage, reduced to the input, does not exceed 0.2-0.3 μ V. In this case the influence of the amplifier noise is decreased due to the transfer coefficient of the transformers.

Figure 2 shows another summator circuit. It contains no transformers, whose fabrication frequently involves technical difficulties. Summation is ensured by the addition of signals of the same phase in a common resistor of the discharge load of the input stages in the field transistors. An identical amplification factor of the stages can be obtained by careful choice of the resistors for the incoming current. The use of field transistors makes it possible to obtain a low noise level and affords a possibility for varying the input resistances of the summator in a broad range. This requires that resistors of a corresponding value be cut in at the inputs.

The necessary additional amplification is ensured by two stages and an emitter follower is cut in at the output. In order to limit the frequency characteristic in the direction of the low frequencies, which are characterized by an increased noise level, it is desirable that the input resistance of the amplifier be decreased, cutting in additional resistors at the input. The choice of these resistors is governed by the output resistance of the string of piezoelectric detectors. If a small number of pressure detectors is used in it, and the output resistance is great, these resistors are excluded.

The amplification of the circuit shown in Fig. 2 is 2000 if two cophasal signals are fed to the appropriate inputs. The noise voltage, reduced to the input, is 1-2 μ V if the input transistors are carefully selected. The frequency band falls in the range 20-2000 Hz.

FOR OFFICIAL USE ONLY

The two amplifiers were checked under expeditionary conditions and good results were obtained.

The use of two strings of piezoelectric detectors in the CSP process, each being towed on different sides of the ship, makes possible some reduction in the noise background and an increase in the signal-to-noise ratio, which favors an increase in the effective depth of the investigations.

BIBLIOGRAPHY

1. Kalinin, A. V., Kalinin, V. V., Fataliyev, M. Kh., "New Method for Seismic Prospecting of Shallow Depths at Sea," VESTNIK MGU, SER. 4 (Herald of Moscow State University, Series 4), No 1, pp 92-95, 1966.
2. Kuzmin, V. A., Sorokhtin, O. G., Sagalevich, A. M., Shekhvatov, B. V., "System for Continuous Seismic Profiling With an Electrosark Source," TRUDY MGI AN UkrSSR (Transactions of the Marine Hydrophysical Institute Ukrainian Academy of Sciences), Sevastopol', pp 259-262, 1972.
3. Lunarskiy, G. N., O VYBORE SOGLASUYUSHCHIKH USTROYSTV DLYA SEYSMICHESKIKH P'YEZOKOS (Choice of Matching Devices for Strings of Seismic Piezoelectric Detectors), Institute of Oceanology USSR Academy of Sciences, Moscow, pp 2-18, 1976 (All-Union Institute of Scientific and Technical Information, No 2870-76 DEP).
4. Neprochnov, Yu. P., SEYSMICHESKIYE ISSLEDOVANIYA V OKEANE (Seismic Investigations in the Ocean), Moscow, Nauka, 1976.
5. Hersey, J. B., "Continuous Reflection Profiling," THE SEA, Vol 3, N. Y., Interscience, pp 47-72, 1963.
6. Ewing, J., Ewing, M., "Seismic Reflection," THE SEA, Vol 4, Part 1, New York, Interscience, pp 1-84, 1970.

COPYRIGHT: Izdatel'stvo "Nauka", "Okeanologiya", 1981
[88-5303]

5303
CSO: 1865

FOR OFFICIAL USE ONLY

TERRESTRIAL GEOPHYSICS

UDC 550.34

SEISMIC INVESTIGATIONS OF THE LITHOSPHERE IN THE PACIFIC OCEAN

Moscow SEYSMICHESKIYE ISSLEDOVANIYA LITOSFERY TIKHOGO OKEANA in Russian 1980 (signed to press 28 Oct 80) pp 2-5, 206-207

[Annotation, introduction and table of contents from book "Seismic Investigations of the Lithosphere in the Pacific Ocean", by Sergey Mitrofanovich Zverev and Nataliya Konstantinovna Kapustyan, Izdatel'stvo "Nauka", 600 copies, 208 pages]

[Text] Annotation. The authors of this book examine new results, methodological problems and ways to increase the effectiveness of seismic investigations at sea, and also the problems involved in comparing data when using modern reception methods: hydrophones and three-component bottom seismographs. The results of a detailed interpretation of wave fields registered in the northwestern and central parts of the Pacific Ocean are presented, as well as new information on lithospheric structure. On the basis of an analysis of original and published data the book gives a new generalized seismic model of the crust of an oceanic type.

The book is intended for geologists and seismologists.

Tables 10, figures 108, references 151 (pp 197-204)

Introduction. Seismic methods play a highly important role in investigation of the sedimentary cover, the consolidated earth's crust and upper mantle, that is, the lithosphere of the oceans. Data on the structure and velocity parameters of these layers are of decisive importance both for creating theoretical concepts concerning the origin and development of the oceans and for such strictly practical problems as an evaluation of the prospects for the production of minerals on the floor of the seas and oceans. Precisely the practical aspect of the problem led to a rapid development of the method and techniques for geophysical investigations at sea.

Against a background of relatively great volumes of schematic investigations of the earth's crust in the oceans by the refracted waves method, individual examples have now appeared of the use of new methodological procedures in the ocean which are partially based on the introduction of seismic prospecting methods and partially related to the development of specific investigations of the oceanic lithosphere. These new methodological procedures in the long run in some cases will lead to new directions in research and fundamentally new results. The use of self-contained bottom seismic stations have broadened the possibilities for deep seismic sounding (DSS) of the earth's crust in the oceans. Detailed observations with full systems

FOR OFFICIAL USE ONLY

FOR OFFICIAL USE ONLY

and long travel-time curves of refracted waves made it possible to clarify the fine structure of the crust of oceanic basins and additional high-velocity discontinuities in the part of the ocean mantle above the asthenosphere. The use of the reflected waves method in the common deep point method made it possible to establish a complex undulating character of the principal discontinuities in the earth's crust and their variability and to determine the details of structure of such complex zones as abyssal trenches in the ocean.

Many of the enumerated methodological innovations have been used in a study of the oceans by Soviet scientists from different organizations, including from the Institute of Physics of the Earth imeni O. Yu. Shmidt USSR Academy of Sciences. From the very beginning the deep seismic sounding method at sea, carried out by the Institute of Physics of the Earth, differed from schematic foreign investigations in having a close tie-in with surface investigations on the continents. Hence the broad use of full systems of observations, land-sea observations, extensive areal investigations of complex zones. On the whole these results are far more saturated with information and are more reliable than the large-scale but schematic observations of foreign investigators which have frequently been based on individual short travel-time curves. The close connection to land seismic investigations is also expressed in the interpretation method, which is more complete and which is based both on the kinematics of systems of counter and overtaking travel-time curves, as well as the dynamics of the principal waves, developed at the Institute of Physics of the Earth by the school of G. A. Gamburtsev and I. S. Berzon.

The great volumes of investigations carried out by the Institute of Physics of the Earth in the oceans were concentrated in complex zones: the transition zone from the Asiatic continent to the Pacific Ocean, Sakhalin-Hokkaido-Primor'ye zone, in the North Atlantic (near Iceland), in individual polygons in the Pacific Ocean; all this also exerted an influence on approaches to methods for making observations and interpretation of materials.

This monograph includes materials having primarily methodological importance for the development of seismic methods for investigating the earth's crust and deeper parts of the lithosphere in the oceans.

Chapter 1 in the monograph examines the conditions for the excitation of seismic waves by means of explosive shots and pneumatic sound sources. In the case of shots, theoretical estimates are given of the parameters, their seismic effectiveness is determined and theoretical and experimental data on the frequency and amplitude characteristics of the excited seismic waves are compared. The possibility of theoretical estimates of the source intensity makes it possible to predict the absolute level of the excited seismic waves of a known nature. This opens up the possibility of using the absolute level of the amplitudes of seismic waves as an additional criterion in establishing their nature.

Nonexplosive sources are examined from the point of view of their intensity and operating stability. Special investigations show that under definite controlling conditions pneumatic sources can give an extremely stable pulse, which makes them promising not only for investigations of the structure of the upper part of the

FOR OFFICIAL USE ONLY

FOR OFFICIAL USE ONLY

earth's crust, but also for the accumulation of signals, necessary in a study of the deep layers of the earth's crust and the top of the mantle.

Chapter II gives an analysis of the peculiarities of registry of seismic waves in the ocean by hydrophones and seismographs. A general solution was obtained for the relationships between all the pressure and other components involved in velocity of displacement of particles, in the simplest case known earlier. On the basis of a study of these relationships it was found to be possible to study the seismic properties of the upper part of the section. The chapter gives the results of processing of experimental data obtained using a three-component bottom station and a hydrophone in different regions of the ocean. Also included is a summary of experimental data on the use of a hydrophone and seismic detector in the registry of seismic waves in the ocean and on the effectiveness of different observation methods in deep seismic investigations of the lithosphere (using bottom stations, self-contained drifting buoys, from submarines). An evaluation of the effectiveness of different observation methods makes it possible to indicate the principal technical solutions for investigating the oceanic lithosphere. These are drifting buoy stations for reconnaissance investigations and schematic study of the earth's crust (using explosive shots and pneumatic sources) and bottom stations when making more detailed investigations with full observation systems and study of great depths in the lithosphere.

A considerable part of the monograph (Chapter III) is devoted to an analysis of wave fields excited by shots and pneumatic sources in a study of the oceanic lithosphere. Material from detailed investigations of the floor of the northwestern part of the Pacific Ocean is set forth in detail. In these investigations for the first time it was possible to obtain reliable data on the presence of a high-velocity discontinuity in the upper mantle below the Mohorovicic discontinuity. An analysis of the kinematic and dynamic characteristics of the wave fields made it possible to determine the nature of seismic waves and to carry out a separation of the earth's crust and upper mantle into blocks in which there is a change in the seismic parameters determining the dynamics of the waves. Typical examples of the registry of waves in the regions of the initial and limiting points were obtained. One section gives representative examples of seismograms, travel-time curves, amplitude and frequency curves, enabling the reader to compare them with his own data.

The chapter describes seismic wave fields for the regions of Marcus Island and Eauripik Plateau (western part of the Pacific Ocean). These investigations, carried out jointly with American and Japanese scientists, are characterized by the simultaneous use of three-component bottom seismic detectors with surface hydrophones of radiobuoys and also spatial observation systems. A peculiarity of one of the sections is the discrimination of a new layer at the bottom of the oceanic earth's crust characterized by a velocity of 7.6 km/sec.

The results of analysis of experimental data, together with published data on the principal parameters of the oceanic lithosphere, made it possible in Chapter IV of the monograph to examine theoretical wave fields for a generalized seismic model of a crust of the oceanic type -- the crust of abyssal oceanic basins -- the simplest and most widely occurring structural form in the ocean. According to modern data, the oceanic lithosphere typically is substantially more stratified than was assumed earlier: the sediments and second layer can be subdivided into several

FOR OFFICIAL USE ONLY

FOR OFFICIAL USE ONLY

intercalations; a new high-velocity layer (velocity more than 7.4 km/sec) is stably present at the bottom of the crust above the Mohorovicic (M) discontinuity. The region of transition from the crust to the mantle can be described both by a quite simple law of change of velocity with depth and can be represented by a complex thin-layered inversion zone. In the upper mantle there can be an additional high-velocity boundary under the M discontinuity. Computations of synthetic seismograms and a detailed interpretation of the kinematic and dynamic characteristics of theoretical wave fields were carried out for the enumerated new data on structure of the lithosphere, reflected in a generalized seismic model at a modern level. On this basis recommendations were given on a method for formulating and carrying out a modern seismic experiment intended for a detailed investigation of structure of the oceanic lithosphere.

The final section in the monograph (Chapter V) is devoted to an examination of modern concepts concerning the lithosphere in the Pacific Ocean and the prospects of its study.

TABLE OF CONTENTS

Introduction..... 3

Chapter I. Characteristics of Excitation of Oscillations Using Shots and Pneumatic Sources..... 6

 Evaluations of Parameters Determining Seismic Effectiveness of Shots..... 6

 Use of Evaluations of Spectral Density of Source in a Comparison of Theoretical and Experimental Amplitude Curves of Seismic Waves..... 9

 Experimental Data on the Frequency and Amplitude Characteristics of Deep Seismic Waves From Underwater Shots..... 15

 Characteristics of Nonexplosive Sources of Oscillations..... 16

Chapter II. Registry of Seismic Waves by Hydrophones and Seismographs..... 22

 Formulation of Problem, Fundamental Equations and Boundary Conditions..... 24

 Relationships of Velocities and Pressures in Dependence on Angles of Emergence of Reflected and Refracted Waves..... 28

 Relationships of Amplitudes of Monotypic Waves Registered by ADSS and ABSS Seismic Stations..... 30

 Comparison of Amplitudes of Waves of Different Types on One Record..... 35

 Examples of Comparison of Fields of Vertical and Horizontal Components of Seismograph..... 38

 Influence of Water Surface on Relationship of Pressure and Velocity..... 47

 Some Experimental Data on the Use of Pressure and Velocity Detectors in Seismic Investigations at Sea..... 48

 Effectiveness of Different Methods for Observing Seismic Waves in Deep Seismic Sounding at Sea..... 50

Chapter III. Analysis of Wave Fields for the Earth's Crust of the Ocean Floor, Continental Slope and Some Rises in the Pacific Ocean..... 55

 Detailed Investigations of the Continental Slope Region and Floor of the Northwestern Part of the Pacific Ocean..... 55

 General Properties of the Wave Field..... 57

 P^K Waves and Characteristics of "Oceanic" Layer of Earth's Crust..... 74

FOR OFFICIAL USE ONLY

PgKp Waves, Transverse in the Earth's Crust of the Ocean, and
Evaluation of the Properties of the "Second Layer"..... 83

P^M Waves and Characteristics of the Structure and Properties of the
Upper Mantle in the Ocean..... 88

General Results of Analysis of the Seismic Wave Field..... 105

Wave Field in the Ocean Floor in the Neighborhood of Marcus Island and
in the Eauripik Plateau..... 106

Chapter IV. Wave Fields for a Generalized Seismic Model of a Crust of the
Oceanic Type..... 116

Generalized Seismic Model of a Crust of the Oceanic Type..... 119

Wave Fields for Different Variants of a Generalized Model..... 128

Dynamic Characteristics of the Fine Structure of the Region of Transition
From the Crust to the Upper Mantle..... 156

Chapter V. Modern Concepts Concerning the Lithosphere of the Pacific Ocean
and Prospects for its Study..... 172

Results of Study of the Earth's Crust in the Pacific Ocean..... 173

Investigations of the Ocean Lithosphere on Long Deep Seismic Sounding
Profiles..... 177

Extent of Occurrence of High-Velocity Layers in the Pacific Ocean
Lithosphere..... 188

Problems in Seismic Investigations of the Pacific Ocean Lithosphere..... 191

Conclusion..... 192

Bibliography..... 198

COPYRIGHT: Izdatel'stvo "Nauka", 1980
[89-5303]

5303
CSO: 1865

FOR OFFICIAL USE ONLY

PHYSICS OF ATMOSPHERE

MODELING OF PHYSICAL PROCESSES IN THE POLAR IONOSPHERE

Apatity MODELIROVANIYE FIZICHESKIKH PROTSESSOY V POLYARNOY IONOSFERE in Russian 1979
(signed to press 15 Dec 79) pp 141, 143-147

[Table of contents and abstracts from collection "Modeling of Physical Processes in the Polar Ionosphere", edited by Ye. A. Mikhaylova, Uchastok Operativnoy Poligrafii Ordena Lenina Kol'skogo Filiala im. S. M. Kirova AN SSSR, 250 copies, 147 pages]

[Text]

TABLE OF CONTENTS

Mizun, Yu. G. "Dynamics of the Polar Ionosphere".....	3
Vlaskov, V. A., Mingalev, V. S., Mingaleva, G. I., Mizun, Yu. G., Parfenova, T. A. "Modeling of the Horizontal Structure of the Polar Ionosphere".....	43
Mingaleva, G. I. "Heating of Ionospheric Plasma as a Result of Elastic Collisions of Particles".....	56
Osepyan, A. P., Smirnova, N. V. "Modeling of Conditions in the Magnetosphere and Ionosphere During Sudden Commencements of World Geomagnetic Storms".....	61
Vlaskov, V. A., Mingalev, V. S. "Electric Fields and Neutral Winds in the High- Latitude Ionosphere".....	71
Mingaleva, G. I. "Role of Mechanisms of Cooling of Thermal Electrons in the Polar Ionosphere".....	76
Smirnova, N. V., Vlaskov, V. A. "Atomic Oxygen in the Disturbed High-Latitude Ionospheric D-Region".....	82
Petrova, G. A. "Effective Coefficient of Losses Under Polar Absorption Conditions".....	98
Ivanov, G. A. "Evaluation of the Effectiveness of a Criterion for a Given Auroral Classification".....	106
Ivanov, V. Ye. "Characteristics of Fluxes of Electrons Backscattered by the Earth's Atmosphere in the Energy Region of Primary Electrons 0.1-1 KeV".....	113
Solodovnikov, G. K. "Wave Disturbances in the Polar Ionosphere".....	130

FOR OFFICIAL USE ONLY

FOR OFFICIAL USE ONLY

Abstracts

UDC 550.388

DYNAMICS OF THE POLAR IONOSPHERE

[Abstract of article by Mizun, Yu. G.]

[Text] This is a review of dynamics of the polar ionosphere. The author gives basic experimental information on movements of electron-ion and neutral gases in the high latitudes. Also considered are the physical reasons for the movements. The role of the dynamics of the polar ionosphere in the distribution of the electron concentration in the high latitudes is discussed. Figures 17, references 66.

UDC 550.338.2

MODELING OF THE HORIZONTAL STRUCTURE OF THE POLAR IONOSPHERE

[Abstract of article by Vlaskov, V. A., Mingalev, V. S., Mingaleva, G. I., Mizun, Yu. G., Parfenova, T. A.]

[Text] The problem of modeling of the horizontal structure of the polar ionosphere is considered on the basis of solution of spatially one-dimensional nonstationary systems of equations with allowance for the convection of plasma. With stipulated models of electric fields, neutral winds and fluxes of auroral particles the authors have obtained the distributions of the electron concentration at different levels in the ionospheric F layer. It is shown that different models of the electric field, all other conditions being equal, give quantitatively different distributions of the electron concentration. Figures 6, references 19.

UDC 551.510.535

HEATING OF IONOSPHERIC PLASMA AS A RESULT OF ELASTIC COLLISIONS OF PARTICLES

[Abstract of article by Mingaleva, G. I.]

[Text] A study was made of heating of ionospheric plasma as a result of elastic collisions of particles caused by the great relative velocities of components of the gas mixture. The examination is made for two models of particle interaction: Maxwellian molecules and small solid spherules. The investigation is made by numerical solution of a system of modeling equations dependent on time, consisting of the thermal conductivity equations for ions and electrons. Figures 2, references 8.

FOR OFFICIAL USE ONLY

UDC 550.388

MODELING OF CONDITIONS IN THE MAGNETOSPHERE AND IONOSPHERE DURING SUDDEN COMMENCEMENTS OF WORLD GEOMAGNETIC STORMS

[Abstract of article by Osepyan, A. P., Smirnova, N. V.]

[Text] On the basis of spectra of trapped electrons measured on the OGO-3 satellite in the nighttime magnetosphere with $K_p = 0-2$ at the L-shell corresponding to the latitude of Loparskaya observatory ($L = 5.3$) and values of the field jump ΔB caused by SC, the authors have computed the differential spectra of trapped electrons in the equatorial plane of the magnetosphere and the spectra of leaking electrons at an altitude of 100 km with different particle lifetimes T_L . For these spectra the article gives computations of the rate of ion formation and using a simplified six-ion model of the D-region the electron density profile and absorption are determined. The resulting absorption values are compared with the absorption measured at Loparskaya ($\Phi = 64.3$ N, $\Lambda = 115.6^\circ$) during SC. For cases of satisfactory agreement with experimental data it was possible to determine the coefficients of diffusion of electrons by pitch angles D , which are compared with the D values obtained under similar conditions in the magnetosphere by other methods. Figures 4, tables 2, references 27.

UDC 550.338.2

ELECTRIC FIELDS AND NEUTRAL WINDS IN THE HIGH-LATITUDE IONOSPHERE

[Abstract of article by Vlaskov, V. A., Mingalev, V. S.]

[Text] This article is devoted to an investigation of the electric field and velocity of the neutral wind in the high-latitude ionosphere during the period of development of a disturbance. It is shown by a comparison of ionosonde data with the results of model computations on an electronic computer that the zonal component of the electric field has a different sign inside and outside the auroral oval, whereas the meridional component of the neutral wind changes its sign with transition from the equinox to summer. Figures 2, references 6.

UDC 551.510.535

ROLE OF MECHANISMS OF COOLING OF THERMAL ELECTRONS IN THE POLAR IONOSPHERE

[Abstract of article by Mingaleva, G. I.]

[Text] This investigation is devoted to a study of the role of different mechanisms of cooling of thermal electrons in the polar ionosphere associated with their inelastic interactions with neutral particles. The author studied the mechanisms of cooling of thermal electrons associated with the transfer of energy to the rotational and vibrational excitation of neutral molecules and also to electron and fine-structural excitation of neutral atoms. The investigation is made by numerical solution of a time-dependent system of modeling equations consisting of the continuity equation for charged particles and the thermal conductivity equations for ions and electrons. Figures 4, references 3.

45

FOR OFFICIAL USE ONLY

FOR OFFICIAL USE ONLY

UDC 551.510.535

ATOMIC OXYGEN IN THE DISTURBED HIGH-LATITUDE IONOSPHERIC D-REGION

[Abstract of article by Smirnova, N. V., Vlaskov, V. A.]

[Text] A study was made of the role of atomic oxygen O in the ion chemistry of the nighttime high-latitude D-region. The authors evaluate the influence of different [O](h) models on the ion composition and profile of electron concentration in the D-region. A justification is given for using a model of increased concentrations of atomic oxygen under the disturbed conditions of leakage of high-energy particles. It is shown that the decrease in the relative content of positive ionic bonds observed under disturbed conditions can be attributed to the simultaneous decrease in the effectiveness of both channels for the formation of ionic bonds from NO^+ and O_2^+ ions with increased concentrations of atomic oxygen. On the basis of the results of computations using a Mitra six-ion scheme for specific polar absorption, AA and SC events it is concluded that in order to describe the behavior of the nighttime high-latitude D-region under conditions of different degrees of disturbance it is necessary to use different [O](h) models. For example, for the reproduction of slightly disturbed conditions good results are given by a model of small [O](h), whereas for the reproduction of more disturbed conditions -- a model of high [O](h). Figures 5, tables 4, references 29.

UDC 550.388.2

EFFECTIVE COEFFICIENT OF LOSSES UNDER POLAR ABSORPTION CONDITIONS

[Abstract of article by Petrova, G. A.]

[Text] This is a review of existing models of the ionization-recombination cycle in the ionospheric D-region. Using data from measurements of the intensity of the proton flux on satellites it was possible to carry out computations of the profiles of the rate of ion formation for three polar cap absorption events: 5 February 1965, 25 January 1971 and 2 September 1971. The determined rates of ion formation, and also the electron density values restored on the basis of measurements of riometer absorption at a number of frequencies at Loparskaya station were used in computations of the altitudinal profiles of the effective coefficient of losses ψ . The resulting profiles agree well with the ψ profiles obtained on the basis of rocket measurements of electron density. Figures 3, references 24.

UDC 62-501

EVALUATION OF THE EFFECTIVENESS OF A CRITERION FOR A GIVEN AURORAL CLASSIFICATION

[Abstract of article by Ivanov, G. A.]

[Text] The author proposes a criterion characterizing the quality of the indicators in a stipulated set, computed using a matrix of the closeness between objects in a teaching sample. The article describes an algorithm for optimizing the criterion, based on the random search method. A program for an electronic computer in which the proposed criterion and algorithm are embodied can be used in choosing indicators for characterizing geophysical situations. References 8.

FOR OFFICIAL USE ONLY

FOR OFFICIAL USE ONLY

UDC 550.388.2

CHARACTERISTICS OF FLUXES OF ELECTRONS BACKSCATTERED BY THE EARTH'S ATMOSPHERE
IN THE ENERGY REGION OF PRIMARY ELECTRONS 0.1-1 KeV

[Abstract of article by Ivanov, V. Ye.]

[Text] The integral and differential characteristics of fluxes of albedo electrons are computed and investigated. The transfer process was modeled using the Monte Carlo method within the framework of a scheme of individual collisions in a three-component medium (O, O₂, N₂). The fluxes of albedo electrons at pitch angles $\approx 0^\circ$ attain 1.6-30% of the intensity of the primary beam in the entire range of initial energies. A further increase in the initial pitch angles leads to an increase in the relative intensity of backscattering. For different ranges of pitch angles ($\theta_0 < 60^\circ$, $\theta_0 > 60^\circ$) there is a diametrically opposite dependence between the magnitude of the albedo flux and the initial beam energy. The pitch angle distribution, being isotropic with small θ_0 with a mean angle $\sim 135^\circ$, with an increase in the initial pitch angles becomes anisotropic with a mean angle $\sim 115^\circ$. The effect of reflection of primary electrons by the magnetic field begins to be manifested with initial pitch angles greater than 60° . In this case in the angle spectrum of albedo electrons a delta-shaped maximum is formed which is caused by that part of the primary beam which was reflected by the magnetic field. Figures 12, references 16.

UDC 550.388

WAVE DISTURBANCES IN THE POLAR IONOSPHERE

[Abstract of article by Solodovnikov, G. K.]

[Text] This article is a review of studies on wave movements in the polar ionosphere. The author gives the morphological characteristics of moving ionospheric disturbances. Also examined are the physical mechanisms of formation of polar ionospheric disturbances and the localization of their sources. Data are given on the relationship between polar ionospheric disturbances and substorms. Infrasonic waves excited during the supersonic movement of plasma arcs in the auroral zone are discussed. Figures 6, references 40.

COPYRIGHT: Kol'skiy filial AN SSSR, 1979
[74-5303]

5303
CSO: 1865

-END-

FOR OFFICIAL USE ONLY